NAVAL POSTGRADUATE SCHOOL
Monterey, California

THESIS

THERMAL CALIBRATION OF SATELLITE INFRARED IMAGES AND CORRELATION WITH SEA-SURFACE NUTRIENT DISTRIBUTION

by

Vitor Martinho F. Pereira e Silva

June 1982

Thesis Advisor: E. Traganza

Approved for public release; distribution unlimited.

UNCLASSIFIED

SECURITY CLASSIFICATION OF THIS PAGE (When Data Entered)

REPORT DOCUMENTATION PAGE		READ INSTRUCTIONS BEFORE COMPLETING FORM
1. REPORT NUMBER	2. GOVT ACCESSION NO.	3. RECIPIENT'S CATALOG NUMBER
4. TITLE (and Subtitle) Thermal Calibration of Satellite Infrared Images and Correlation with Sea-Surface Nutrient Distribution		5. TYPE OF REPORT & PERIOD COVERED Master's thesis; June 1982 6. PERFORMING ORG. REPORT NUMBER
7. AUTHOR(s) Vitor Martinho F. Pereira e Silva		8. CONTRACT OR GRANT NUMBER(s)
9. PERFORMING ORGANIZATION NAME AND ADDRESS Naval Postgraduate School Monterey, California 93940		10. PROGRAM ELEMENT, PROJECT, TASK AREA & WORK UNIT NUMBERS
11. CONTROLLING OFFICE NAME AND ADDRESS Naval Postgraduate School Monterey, California 93940		12. REPORT DATE June 1982 13. NUMBER OF PAGES 64
14. MONITORING AGENCY NAME & ADDRESS(if different from Controlling Office)		15. SECURITY CLASS. (of this report) Unclassified 15a. DECLASSIFICATION/DOWNGRADING SCHEDULE

16. DISTRIBUTION STATEMENT (of this Report)

Approved for public release; distribution unlimited.

17. DISTRIBUTION STATEMENT (of the abstract entered in Block 20, if different from Report)

18. SUPPLEMENTARY NOTES

19. KEY WORDS (Continue on reverse side if necessary and identify by block number)

satellite infrared imagery; radiative transfer theory; sea surface temperature; nutrients; nitrate; phosphate; upwelling; mapping

20. ABSTRACT (Continue on reverse side if necessary and identify by block number)

Satellite infrared imagery off the California coast, near Pt. Sur, show thermal patterns associated with an upwelling center; the patterns frequently curl cyclonically when interacting with the warmer California Current. This pattern shows sharp thermal fronts, easily identified in satellite IR images, that are strongly correlated with nutrient fronts during the early stages of upwelling. With sea truth data available, it

DD FORM 1 JAN 73 1473 EDITION OF 1 NOV 68 IS OBSOLETE
S/N 0102-014-6601

UNCLASSIFIED
SECURITY CLASSIFICATION OF THIS PAGE (When Data Entered)

#20 - ABSTRACT - (CONTINUED)

was feasible to calibrate satellite derived sea surface temperature, by applying radiative transfer theory, and to infer nutrient concentrations from their linear inverse correlations with temperature. Thus, it was possible to calibrate satellite thermal fields to produce maps of nutrient distributions. When the inferred relationships were applied over representative regions of the upwelling center, standard deviations of 0.5°C, 1.7 μM and 0.1 μM were computed for temperature, nitrate and phosphate, respectively.

Approved for public release; distribution unlimited.

Thermal Calibration of Satellite Infrared Images and Correlation with Sea-Surface Nutrient Distribution

by

Vitor Martinho F. Pereira e Silva
Lieutenant, Portuguese Navy
B.A., Portuguese Naval Academy, 1976

Submitted in partial fulfillment of the requirements for the degree of

MASTER OF SCIENCE IN OCEANOGRAPHY

from the

NAVAL POSTGRADUATE SCHOOL

June 1982

ABSTRACT

Satellite infrared imagery off the California coast, near Pt. Sur, show thermal patterns associated with an upwelling center; the patterns frequently curl cyclonically when interacting with the warmer California Current. This pattern shows sharp thermal fronts, easily identified in satellite IR images, that are strongly correlated with nutrient fronts during the early stages of upwelling. With sea truth data available, it was feasible to calibrate satellite derived sea surface temperature, by applying radiative transfer theory, and to infer nutrient concentrations from their linear inverse correlations with temperature. Thus, it was possible to calibrate satellite thermal fields to produce maps of nutrient distributions. When the inferred relationships were applied over representative regions of the upwelling center, standard deviations of 0.5°C, 1.7 μM and 0.1 μM were computed for temperature, nitrate and phosphate, respectively.

TABLE OF CONTENTS

LIST OF TABLES

LIST OF PHOTOGRAPHIC PLATES

LIST OF FIGURES

ACKNOWLEDGMENTS

The author wishes to thank Dr. Eugene D. Traganza, thesis advisor and principal investigator, whose assistance made this task possible. Sincere appreciation is extended to Dr. James L. Mueller for his assistance and recommendations during this research, Mr. Laurence C. Breaker of the National Environmental Satellite Service at Redwood City, California for his help in obtaining the satellite data, and Mr. Robert Wrigley, of the NASA-Ames Research Center at Moffett Field, California for his assistance in the work with the IDIMS system. Lastly, I would like to thank Isabel, my future wife, for her forbearance and support, although physically away.

I. INTRODUCTION

This thesis is a study of the possibility of calibrating infra-red satellite images from limited in-situ temperature data, and the possibility of whether chemical (specifically nitrate and phosphate concentrations) mesoscale variability may be inferred from corresponding satellite detected thermal patterns in an upwelling zone [Traganza, 1980].

Very high resolution infrared radiometry, with a spatial and amplitude resolution ~1.0 km and ~0.5 °C, respectively, have been successfully used in locating and sensing sea surface temperature contrasts in upwelling zones [Traganza et al., 1980; Bowman et al., 1977]. Due to the development in radiative transfer theory and satellite imagery it is possible to calibrate this satellite derived temperature when sea truth data are available, and the atmospheric moisture distribution is uniform.

Surface temperature and nutrient maps can be generated using these corrected satellite derived temperatures, and nutrient to temperature correlations, because active upwelling systems in an early stage of development are expected to have strong inverse linear correlations between nutrients and temperature. The recurrent formation of "a cyclonic upwelling system" off Pt. Sur, California [Traganza, Conrad and Breaker, 1980] offers a unique opportunity to simultaneously investigate the accuracy of satellite generated surface maps for

temperature and nutrients, and the influence that coastal upwelling has on surface nutrient concentrations when it brings nutrient-rich waters into the euphotic zone. This appears to be a major factor regulating the standing stock and production of phytoplankton in coastal waters [Eppley et al., 1979]. And, because phytoplankton are the primary producers in the pelagic ecosystem, supporting the foodweb, it will be of interest to obtain a wider and instantaneous picture of the nutrient concentrations, which only a satellite can give, although indirectly.

Thermal gradients detected by IR imagery identify potential site of high biomass which may be confirmed by Coastal Zone Color Scanner (CZCS) data [Traganza, 1981]. This data can reveal subtle variations in the concentration of phytoplankton pigments and has a potential application for the study of large-scale patchiness in phytoplankton distributions [Hovis et al., 1980].

II. METHODS

A. CRUISES

Sea truth data were obtained from the cruises conducted aboard the Naval Postgraduate School's research vessel R/V ACANIA on 10 and 11 June 1980 and 29 October 1980.

To ensure coverage of the cyclonic moving feature updated satellite information regarding its approximate location, size, center and orientation, was sent prior to each cruise and sometimes during the cruise by Mr. Breaker, the staff oceanographer at the National Environmental Satellite Service (NESS) Station, in Redwood City, California. R/V ACANIA positions within this "cyclonic upwelling system," centered a few kilometers southwest of Point Sur, were determined by LORAN-C which has good coverage in this region. Temperature and nutrients were measured in situ every two minutes at a depth of 2.5 m. Seawater temperature was sensed by a thermistor, and recorded continuously on a strip chart. For calibration and monitoring of the equipment sea surface temperature was also measured by bucket thermometer. Surface nutrient concentrations were recorded and analyzed every two minutes according to the Technicon Industrial Method [Hanson, 1980].

B. SATELLITE IMAGERY

Three satellite images of the region offshore Central California were analyzed and calibrated. They were chosen

because they were cloud-free over the upwelling feature and taken during or very close to the cruise time.

The infrared (10.5 to 12.5 μM) data recorded in the satellite orbits were analyzed at the NASA-Ames Research Center, in a computer equipped with the Interactive Digital Image Manipulation System (IDIMS), which is a comprehensive software package developed by Electromagnetic Systems Laboratories, Inc. With this software package, the author could "zoom" magnify and pseudo-color the displayed image under "joystick" control. Some 8-by-10 inch color Polaroid prints were taken, as shown in Plates 1, 2 and 3. A computer printout (picprint), with the recorded count values (radiometric units of measurement) was also obtained (Figs. 1, 8, 15). To navigate on it, and because there were no geographical coordinates on the picprint, the author used a computer program developed by Lundell (1980). The purpose of this program is to determine the line and pixel number of a geographical location given the locations latitude and longitude, of a landmark location (line, pixel, latitude and longitude) and the period and inclination of the satellite orbit.

With the image navigational problem solved, it was possible to draw portions of the R/V ACANIA cruise tracks on the picprint in order to compare the digitized satellite temperatures with the in-situ values.

C. INFRARED RADIOMETRY

1. Temperature Degradation

The usefulness of satellite observations depends on the ability of the radiometer to view the sea with little error introduced by the atmosphere. This error, which can be substantial even in a relatively clear air, is mainly induced by atmospheric attenuation of the infrared radiance due to absorption by water vapor. According to Maul and Sidran (1973), this effect varies from small values for arctic atmospheres to fairly high values, ca. 10°C for tropical atmospheres. In mid-latitudes, this attenuation may introduce errors on the order of 2 to 6°C.

Water, both as vapor and as clouds, is the primary source of error. Even in cloud-free atmospheres, where scattering of infrared radiance is negligible, the magnitude of absorption and the variability of the moisture field presents a severe problem. Theoretically, the influence of water vapor can be calculated if the absorption coefficient of water vapor as well as the vertical temperature and humidity profiles are known. However, this requires radiosonde data for a study area, which is rather the exception. Even using an isolated sounding the temperature accuracy is limited to 1°C [Maul and Sidran, 1973].

Failure to detect the increase in humidity, due to clouds, leads to 2 to 5°C errors in the calculations. Even in clear atmospheres, the water vapor can reduce the apparent sea surface temperature by 4 to 8°C. Furthermore, the

presence of moisture markedly attenuates surface temperature gradients across an oceanic front [Maul et al., 1978].

Because the influence of clouds is the most difficult variable to estimate and to correct for, the cloud-free satellite observations, present during this study, minimized the atmospheric errors and simplified the radiative transfer equation because scattering of infrared radiance could be neglected.

Adding to these atmospheric errors and increasing the total deviation between satellite derived temperatues and in-situ temperatures, are errors originating at the sea surface, due to the very strong absorption (a) of infrared photons on it. This produces a very thin optical depth ($z_{1/\ell} = 1/a$), on the order of ca. 0.006 mm for the ca. 10.5 μM to 12.5 μM IR spectral window. As a consequence, the IR radiation measured by the radiometer originates in the upper 0.006 mm of the sea surface, and may not represent slightly deeper temperatures, as those obtained by the thermistor at 2.5 m on the R/V ACANIA cruises. The very thin "skin" at the top of the ocean is in a quasi-laminar viscous sub-layer, dominated by molecular fluxes, which are the reason for the discrepancy between the sea surface temperatures sensed remotely by infrared and by in-situ methods. The difference is usually on the order of ca. 0.5 to 1°C, with the in-situ values warmer [Stewart, 1979].

All these errors originating in the atmosphere and at the ocean surface will be corrected indirectly in this study

by correlation between temperature derived radiances from satellite and in-situ data. The author will assume negligible both water vapor gradient and temperature discrepancy (between satellite derived and in-situ temperatures) gradient within the area.

2. Planck Function

The sea surface emits thermal infrared spectral radiance (L) as a function of the wavelength (λ), the sea surface temperature (T) and zenith incidence angle (θ) according to the equation

$$L(\lambda,\theta,T) = \varepsilon(\lambda,\theta)\cdot\beta(\lambda,T)$$

where $\beta(\lambda,T)$ is the Planck Function,

$$\beta(\lambda,T) = \frac{2hc^2}{\lambda^5\cdot[\exp(hc/kT\lambda)-1]} \text{ Watts}\cdot\text{steradian}^{-1}\cdot\text{m}^{-3}$$

where

h = Planck's constant = 6.626196×10^{-34} joule.sec

λ = wavelength of emitted radiation, meters

c = speed of light = 2.997925×10^{8} m$\cdot$sec^{-1}

k = Boltzmann's constant = 1.380622×10^{-23} joule$\cdot$K^{-1}

T = temperature, K

The Planck Function gives the spectral radiance emitted by an ideal blackbody. However, the sea surface is not an

ideal blackbody and emits less radiation. The factor $\varepsilon(\lambda,\theta)$ accounts for this fact, and is called Emissivity, $\varepsilon(\lambda,\theta)$

$$\varepsilon(\lambda,\theta) = \frac{\beta(\text{sea surface, K})}{\beta(\text{blackbody, K})}$$

Because its averaged value over the IR spectral window (10.5 μm to 12.5 μm) remains near ca. 0.98 for θ ca. 0° to 40°, this value was used in the computations of radiances.

3. Radiative Transfer Theory

Absolute measurements of sea-surface temperature could, in theory, be produced from solutions of the radiative transfer equation,

$$L(T_\lambda) = L_0(T_s)\cdot\tau(p_0) + L_*$$

where

$L(T_\lambda)$ = radiance measured by the satellite radiometer in watts·steradian^{-1}·m^{-3}

T_λ = temperature obtained by inverting the Planck's function for the measured value of radiance in K

$L_0(T_s)$ = total radiance emitted from the surface at temperature T_s in watts·steradian^{-1}·m^{-3}

$\tau(p_0)$ = atmospheric transmittance between the pressure levels ca. 0 (top of the atmosphere) and p_0 (sea level)

L_* = path radiance due to the isotropic thermal emission of photons by the atmosphere along the propagation path from the sea surface to the radiometer in watts·steradian^{-1}·m^{-3}

using detailed atmospheric observations and multi-channel satellite radiometers. In this study, such data were not available, and therefore, a simpler scheme was used of necessity. To derive the parameters τ, the atmospheric transmittance, and L_*, the path radiance, both sets of satellite and in situ temperature observations in the observed frontal zones, where thermal differences are large enough to reduce the relative errors due to satellite measured thermal noise (e.g., caused by variable moisture over the area) and due to a coarse AVHRR (Advanced Very High Resolution Radiometer) temperature resolution of 0.5 °C*. More precisely, linear regression analysis was done on both sets of temperature derived radiances versus elapsed distance along the cruise track, in frontal regions (Figs. 2, 9, and 16). Assuming that the sea surface temperature gradient is much larger than the moisture gradient, then $|\nabla L_0| >> |\nabla L_*|$, then by the radiative transfer equation

$$\tau = \nabla L / \nabla L_0; \quad \tau < 1$$

within a very few percent. The ratio of the slopes of the regression lines will give then, the transmittance, τ. The other atmospheric correction factor in the radiative transfer

---

*Although the inherent quantization of the AVHRR is ~0.2 K at 285 K, the NESS station in Redwood City can only record eight bits of the 10 bits transmitted by the satellite, thus degrading the resolution to 0.5 K in the data available for this study.

equation, the path radiance, L_*, can be estimated using the intercepts with the Y-axis of the satellite and in-situ radiances regression lines, respectively L' and L'_0, knowing that

$$L = m_1 x + L'$$

and

$$L_0 = m_2 x + L'_0$$

where m_1 and m_2 are the slopes of the satellite and in-situ radiance regression lines. Taking in account the relationship between the slopes of both lines, $\tau = m_1/m_2$, and substituting in the radiative transfer equation, the equation for the path radiance is obtained:

$$L_* = L' - \tau \cdot L'_0$$

Finally, knowing both transmittance, τ, and path radiance, L_*, any apparent (measured by the AVHRR) sea surface temperature was corrected for using the radiative transfer equation, with reasonable accuracy (residual std. dev. 0.5°C).

D. LINEAR REGRESSION AND CORRELATION COMPUTATIONS

Least squares linear regressions, designed to minimize the sum of the squares of the deviations of the data points from the straight line of best fit, were performed in nitrate versus phosphate, nitrate versus temperature and phosphate versus temperature. Regression lines were also generated for

radiances, computed from *in situ* and satellite temperatures, versus elapsed distance along the portions of the cruise track with strong temperature gradients and nearest in time to the satellite overpass. The slopes and y-intercepts from the regression lines were computed from the equation

$$m = \frac{\Sigma x_i y_i - N\Sigma x_i y_i}{(\Sigma x_i)^2 - N\Sigma x_i^2}$$

$$b = \bar{y} - m\bar{x}$$

The population correlation coefficient was also computed for the nutrient regression lines, using the equation

$$r = \frac{m\,\sigma_x}{\sigma_y}$$

where σ_x and σ_y are the standard deviations of the x and y values, respectively.

III. RESULTS

A. 9 JUNE 1980 SATELLITE IMAGERY

Several satellite images off Central California prior to and including 9 June, showed a "tongue" of upwelling water within an early stage of development, near Pt. Sur.

The best cloud-free image was taken by the satellite NOAA-6, in its orbit number 4954, at 0250 GMT 9 June 1980. The infrared (10.5 μm to 12.5 μm) data recorded in this orbit was analyzed, at the NASA-Ames Research Center, in a computer equipped with the IDIMS. Plate 1 shows the black and white copy of the pseudo-color image processed. A computer print-out (picprint) with the recorded count values was also obtained. With the identification of several geographical locations (Pt. Sur, Pfeiffer Pt. and Lopez Pt.) and using the computer program developed by Lundell (1980), the portion of the R/V ACANIA cruise track nearest in time to the satellite overpass was drawn on it (Fig. 1). Temperatures were digitized along the cruise track and compared with the *in-situ* values (Fig. 2). Regression lines were computed for both *in-situ* and satellite temperature derived radiances, in the regions with strong gradients, *viz.*, between elapsed distance *ca.* 4 km to 16 km, 30 km to 60 km and 64 km to 83 km. From the comparison between these lines, averaged values for the transmittance *ca.* 0.693 and the path radiance *ca.* 2,150,000 Watts·steradian^{-1}·m^{-3} were computed. Using these values in the radiative transfer

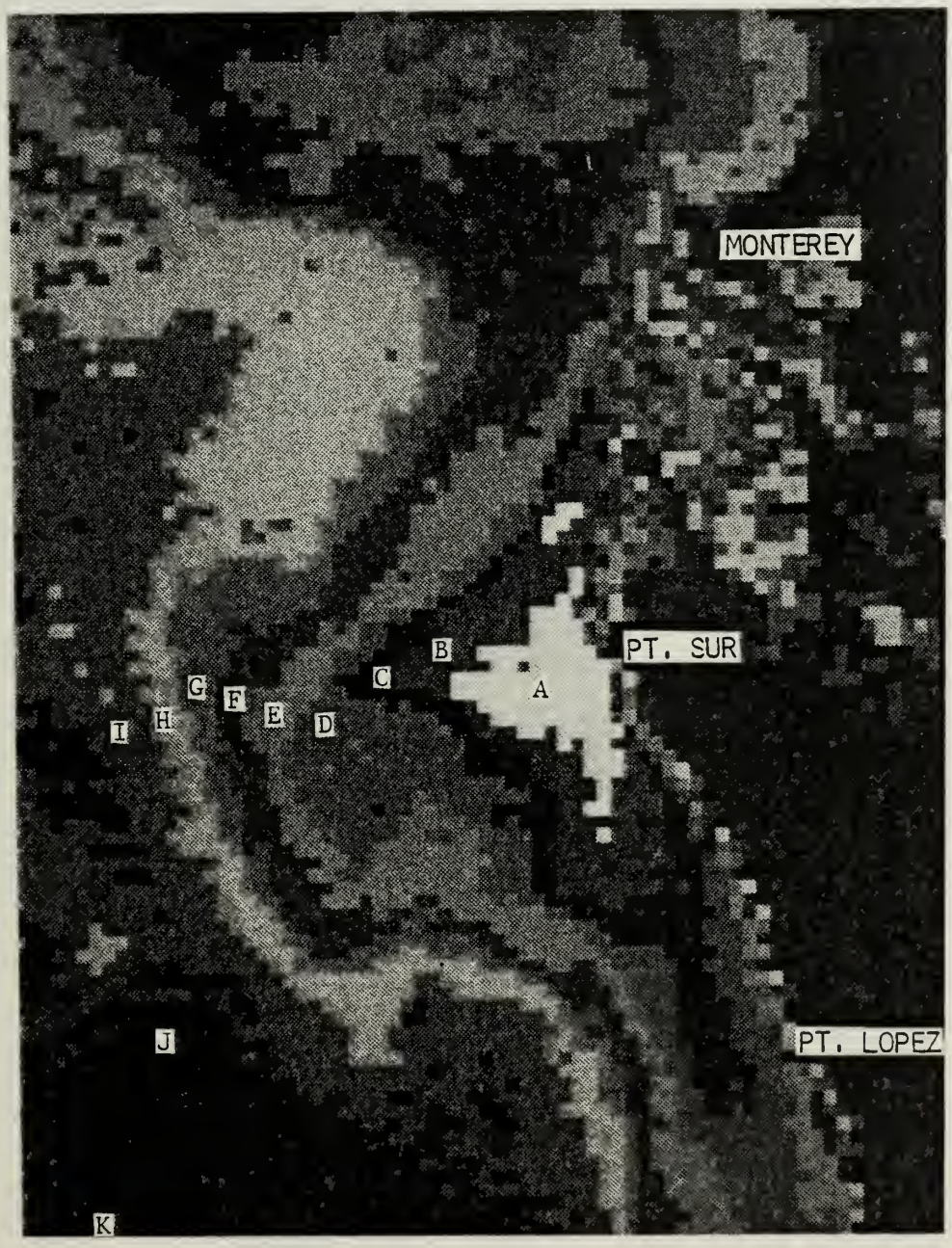

Plate 1. NOAA-6 satellite image of the California coast for 9 June 1980. Letters associated with color grades represent averaged temperatures, over a pixel, measured by the radiometer (see Table I for radiometric count, temperature, nitrate and phosphate values).

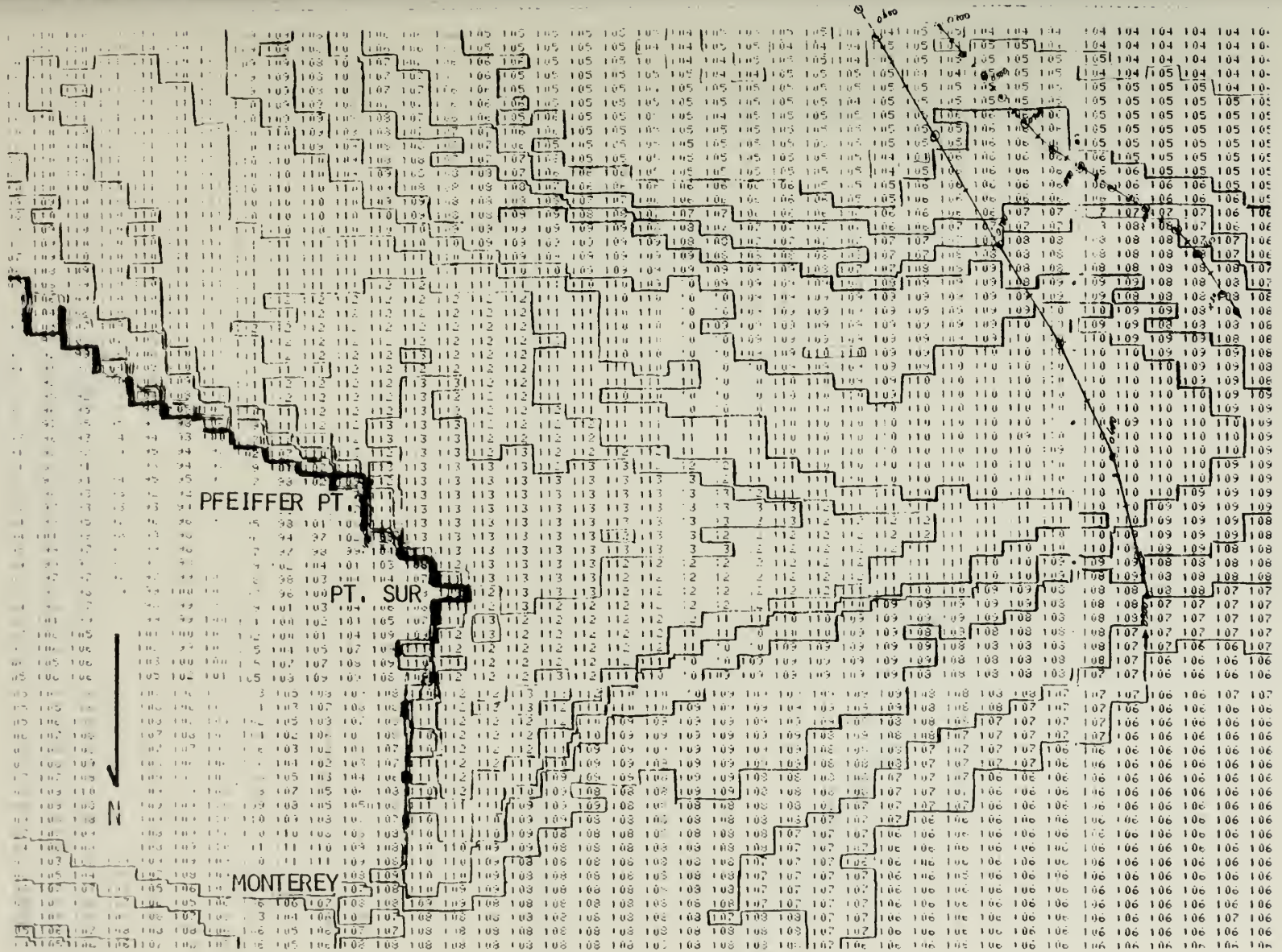

Figure 1. Sample of the picprint of the satellite image for 9 June 1980 with the coast line, thermal isolines and a portion of the June cruise drawn on it

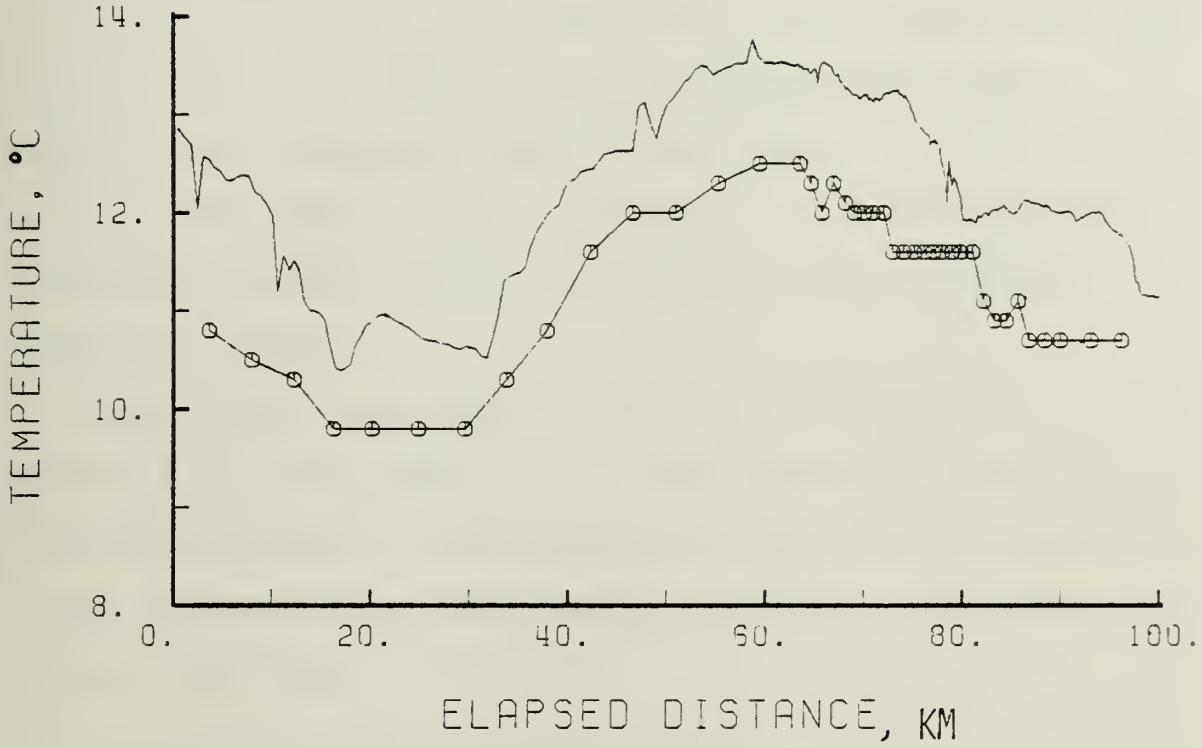

Figure 2. In-situ temperature (straight line) and satellite temperature (line with circles) versus elapsed distance along a portion of the cruise track of the 9-10 June 1980 cruise.

equation it was possible to correct the satellite temperatures associated with the count values (Table I).

The sea surface nutrient distribution was obtained from its correlation with the in-situ thermal distribution. Linear regression analysis between nitrate and temperature, phosphate and temperature, and nitrate to phosphate yielded slopes of -3.55, -0.27 and 12.79 respectively, and y-axis intercepts of 49.27 μM, 4.72 μM and -12.25 μM respectively (Figs. 3, 4 and 5). The correlation coefficients were $r = -0.96$, $r = -0.96$ and $r = 0.98$ respectively. From this analysis a nutrient concentration was computed for each calibrated satellite temperature (Table I).

Sea surface temperature nitrate and phosphate maps were generated by "zoom transfering"* the thermal pattern in the IR satellite image to a navigational chart. Each isopleth is the average of the temperature or nutrient concentration on each side (Figs. 6, 7 and 8).

B. 11 JUNE 1980 AND SATELLITE IMAGERY

A strong "cyclonic upwelling feature" [Traganza, E.D., et al., (1980); Traganza, E.D., Austin, D., (1981)] is shown in the image taken by the satellite NOAA-6, in its orbit number 4983, at 0350 GMT 11 June 1980. Plate 2 shows the black and white copy of the pseudo-color image processed with IDIMS.

---

*This was done using zoom transfer scope, an optical device used to superimpose one magnified and linearly stretched image on another, so that spatial features may be transferred by tracing with a pen.

Table I

Calibration Table of the satellite image for 9 June 1980
(the '*' represents values below limit of detection)

Color Grade	Count	Satellite Temperature (°C)	Corrected Temperature (°C)	Nitrate NO_3^- (μM)	Phosphate PO_4^{3-} (μM)
K	103	12.90	14.92	*	0.69
J	104	12.47	14.31	*	0.85
I	105	12.03	13.68	0.73	1.02
			13.37	1.83	1.11
H	106	11.59	13.06	2.93	1.19
			12.75	4.05	1.28
G	107	11.15	12.43	5.16	1.36
			12.11	6.30	1.45
F	108	10.70	11.79	7.44	1.54
			11.48	8.56	1.63
E	109	10.26	11.16	9.67	1.71
			10.84	10.82	1.80
D	110	9.81	10.51	11.96	1.88
			10.19	13.11	1.97
C	111	9.36	9.87	14.25	2.05
			9.55	15.40	2.14
B	112	8.91	9.22	16.55	2.23
			8.90	17.70	2.32
A	113	8.46	8.57	18.85	2.40

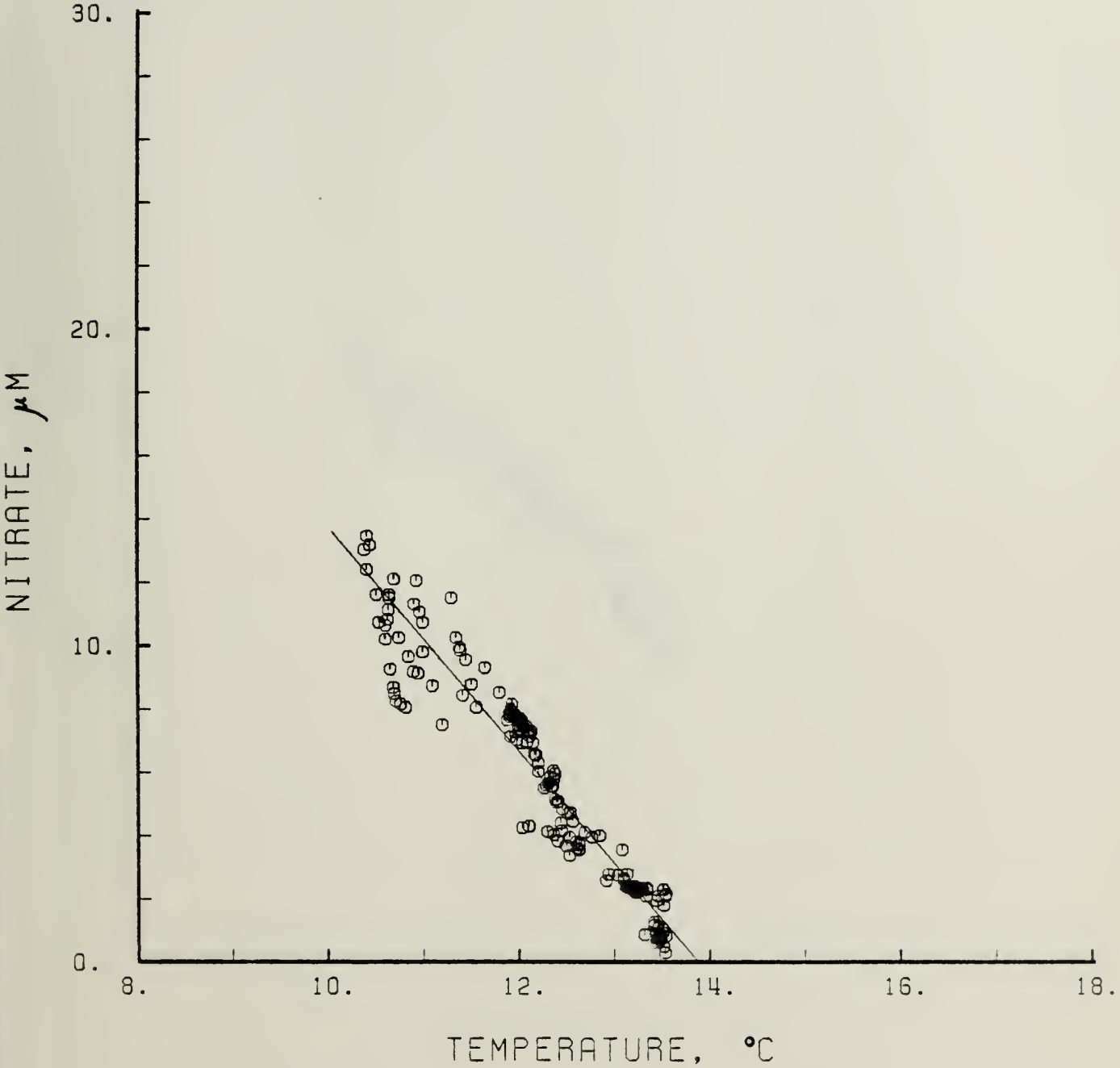

Figure 3. Nitrate versus temperature with the regression line for 10 June 1980.

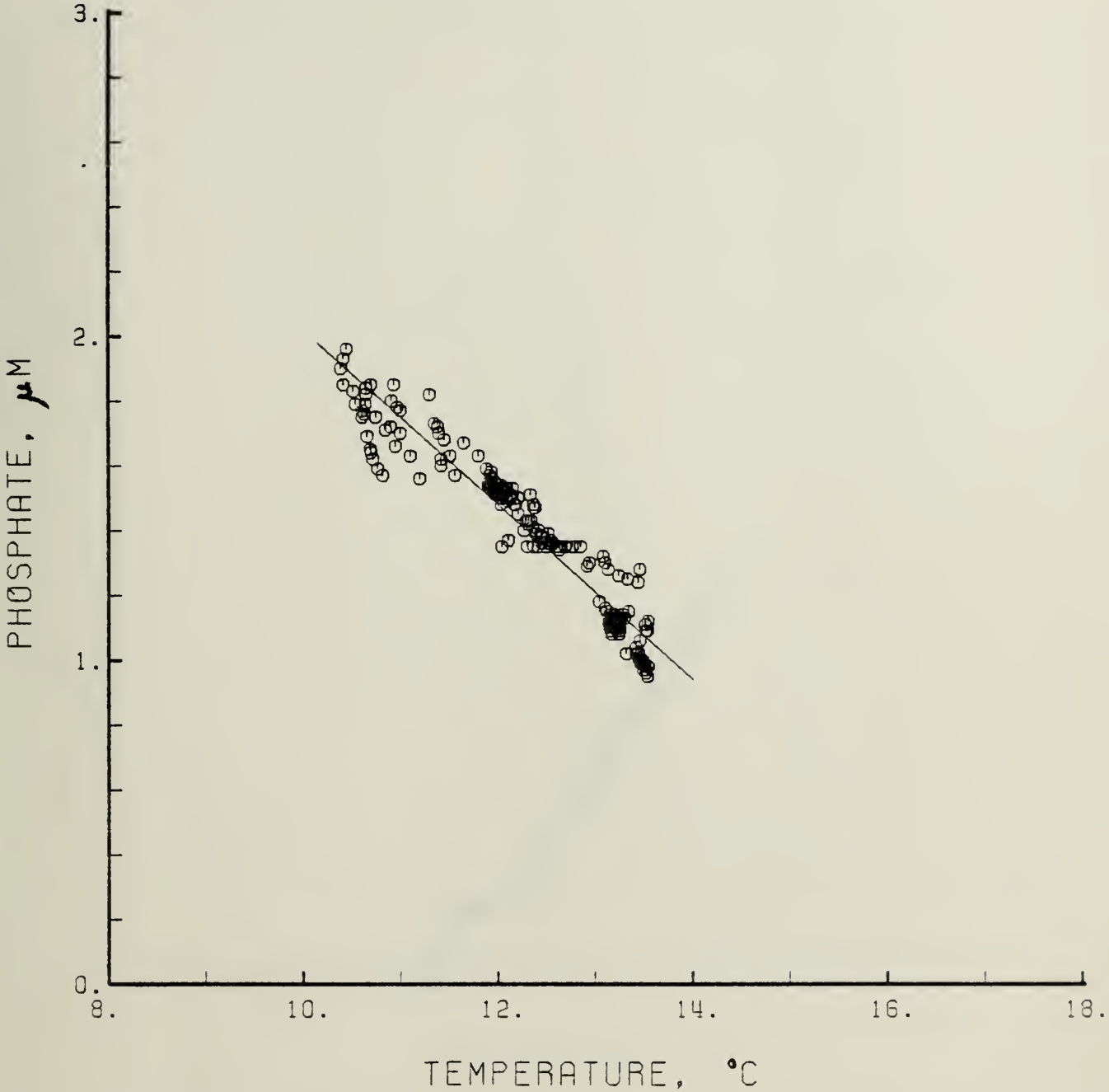

Figure 4. Phosphate versus temperature with the regression line for 10 June 1980.

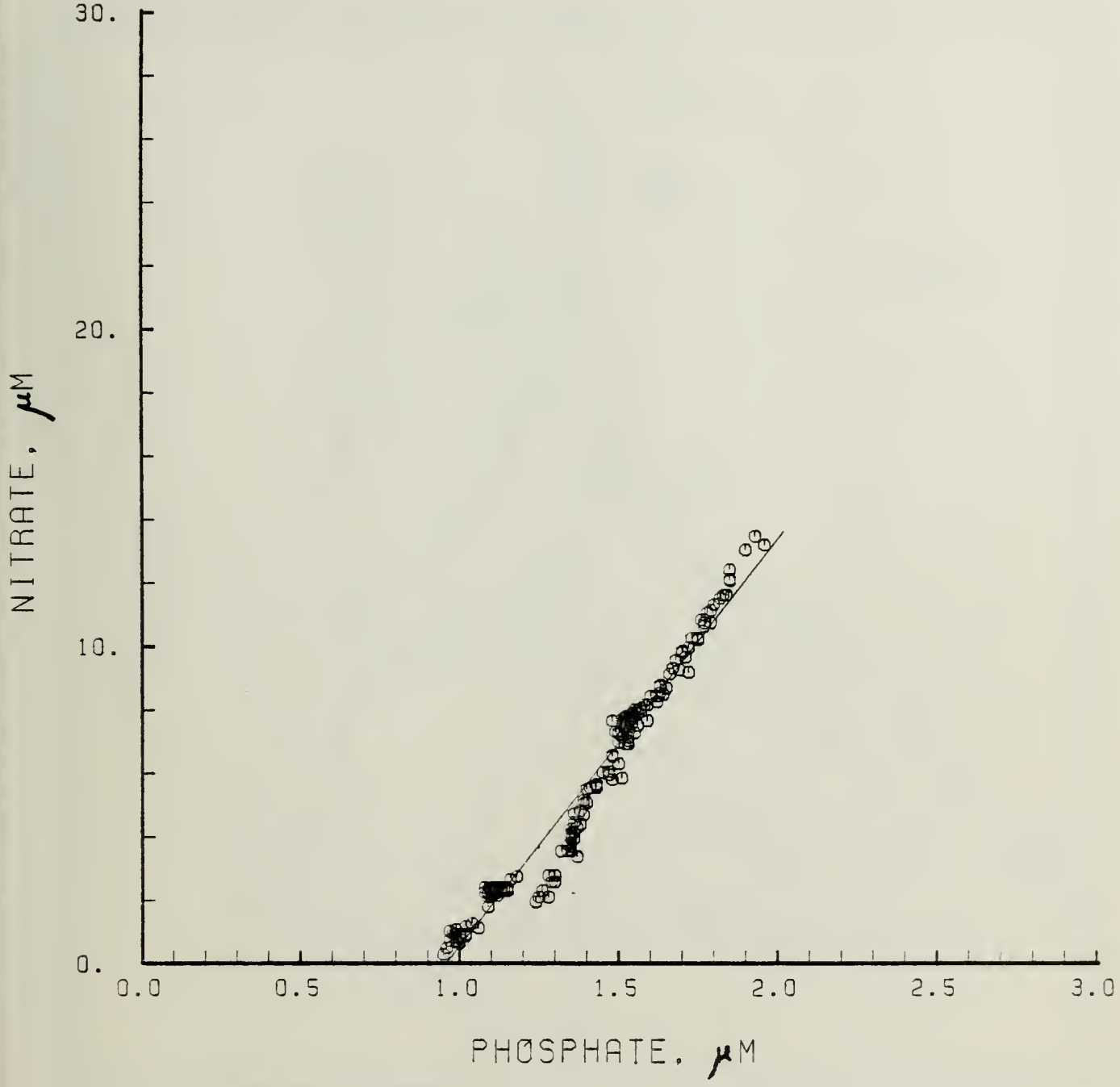

Figure 5. Nitrate versus phosphate with the regression line for 10 June 1980.

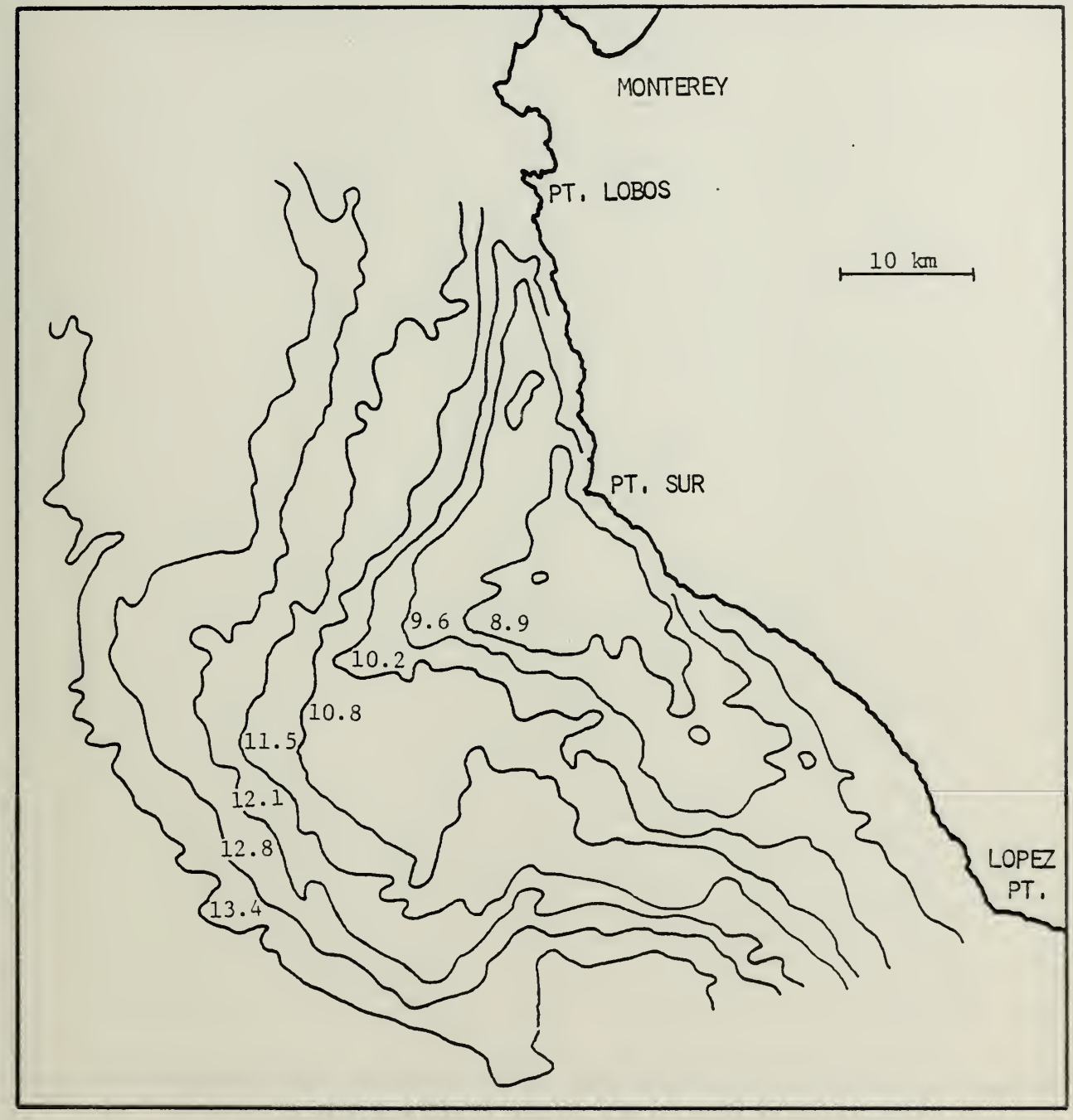

Figure 6. Sea surface temperature maps in °C for 9 June 1980 inferred from satellite IR imagery. Contour interval is one radiometric unit of measurement (1 count ≃ 0.5°C).

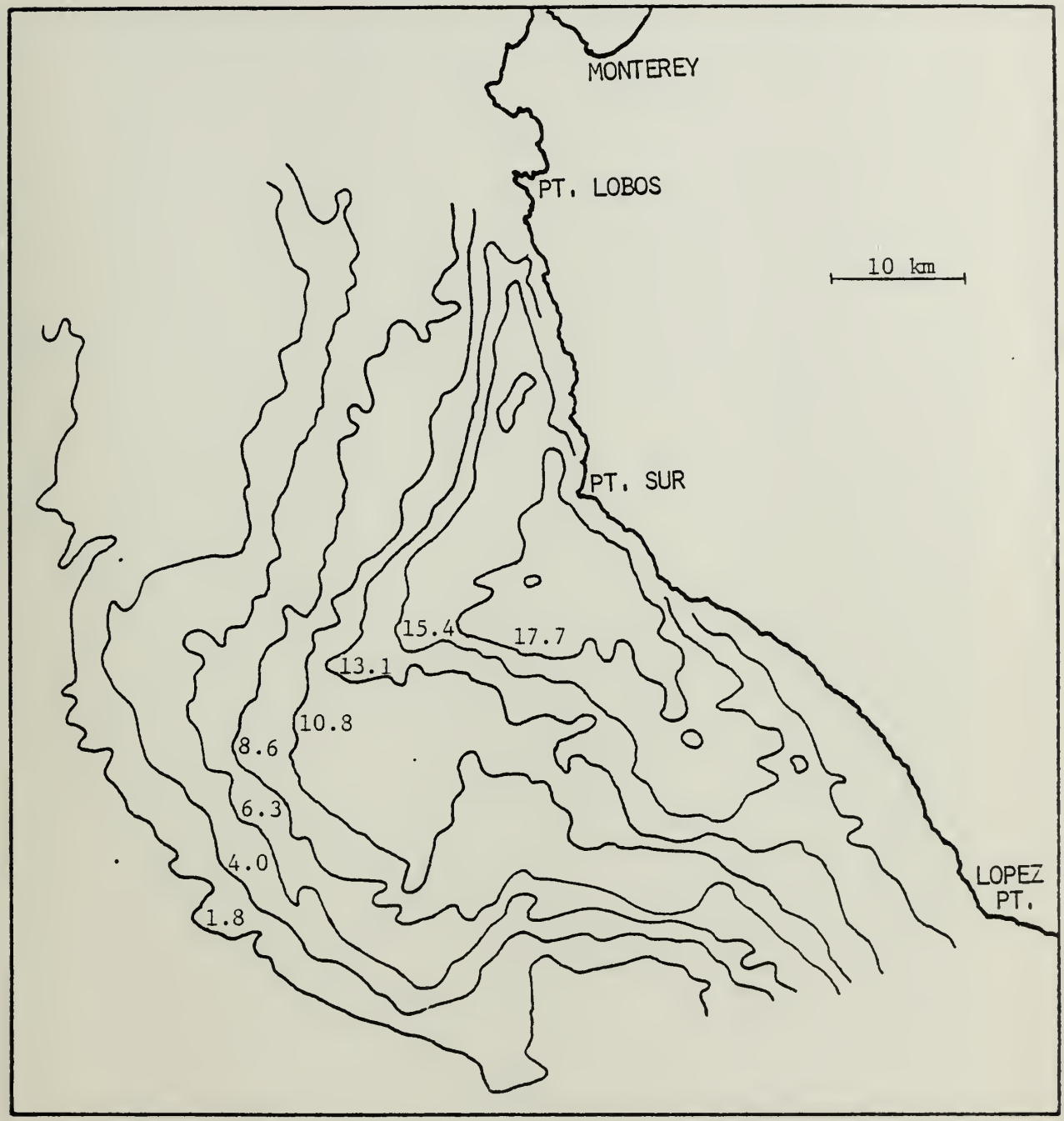

Figure 7. Sea surface nitrate map for 9 June 1980, generated by correlation with sea surface temperature distribution given by IR imagery. Contour interval is one radiometric unit of measurement (1 count ≃ 0.5°C). Nitrate concentrations are given in μM.

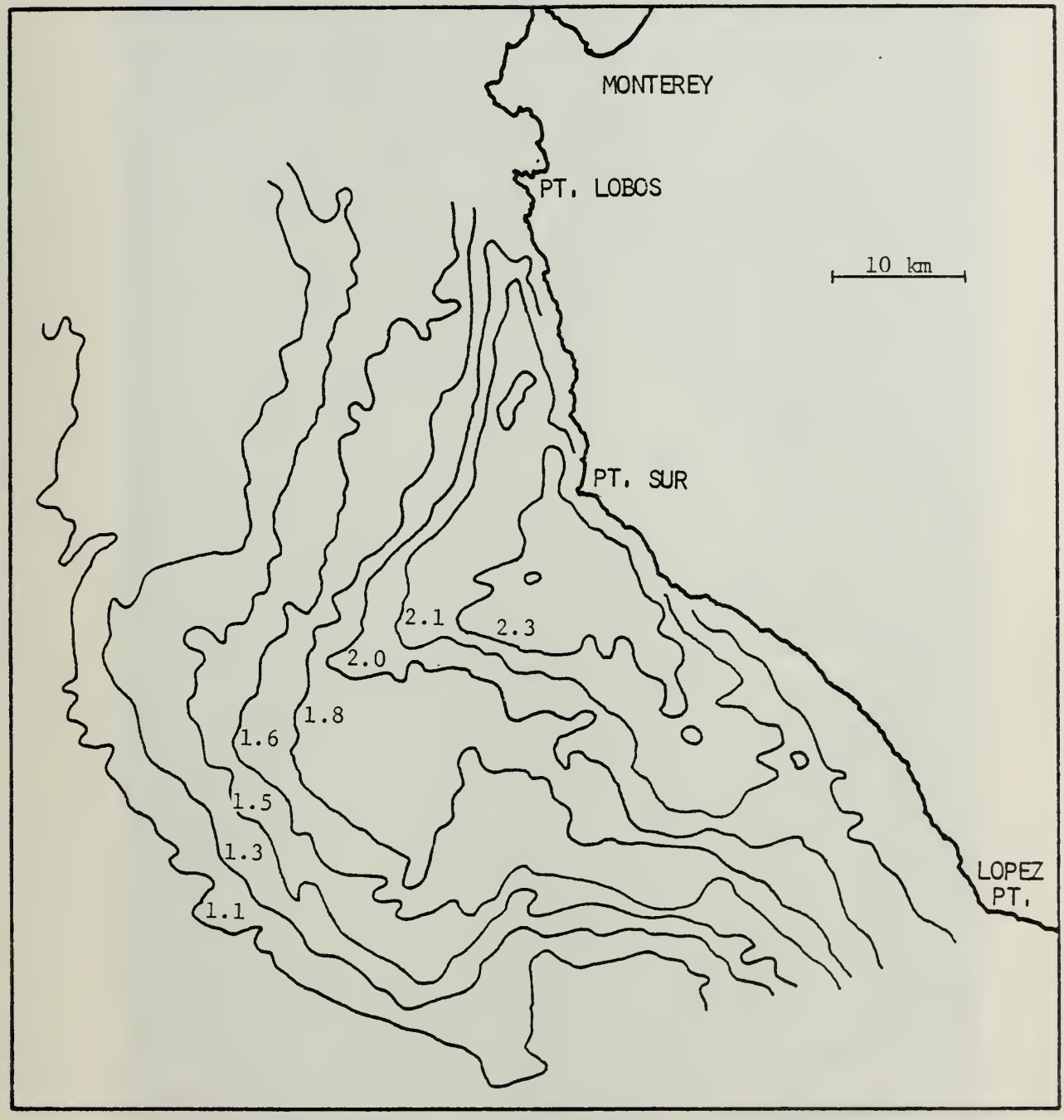

Figure 8. Sea surface phosphate map for 9 June 1980, generated by correlation with sea surface temperature distribution given by IR imagery. Contour interval is one radiometric unit of measurement (1 count ≈ 0.5°C). Phosphate concentrations are given in uM.

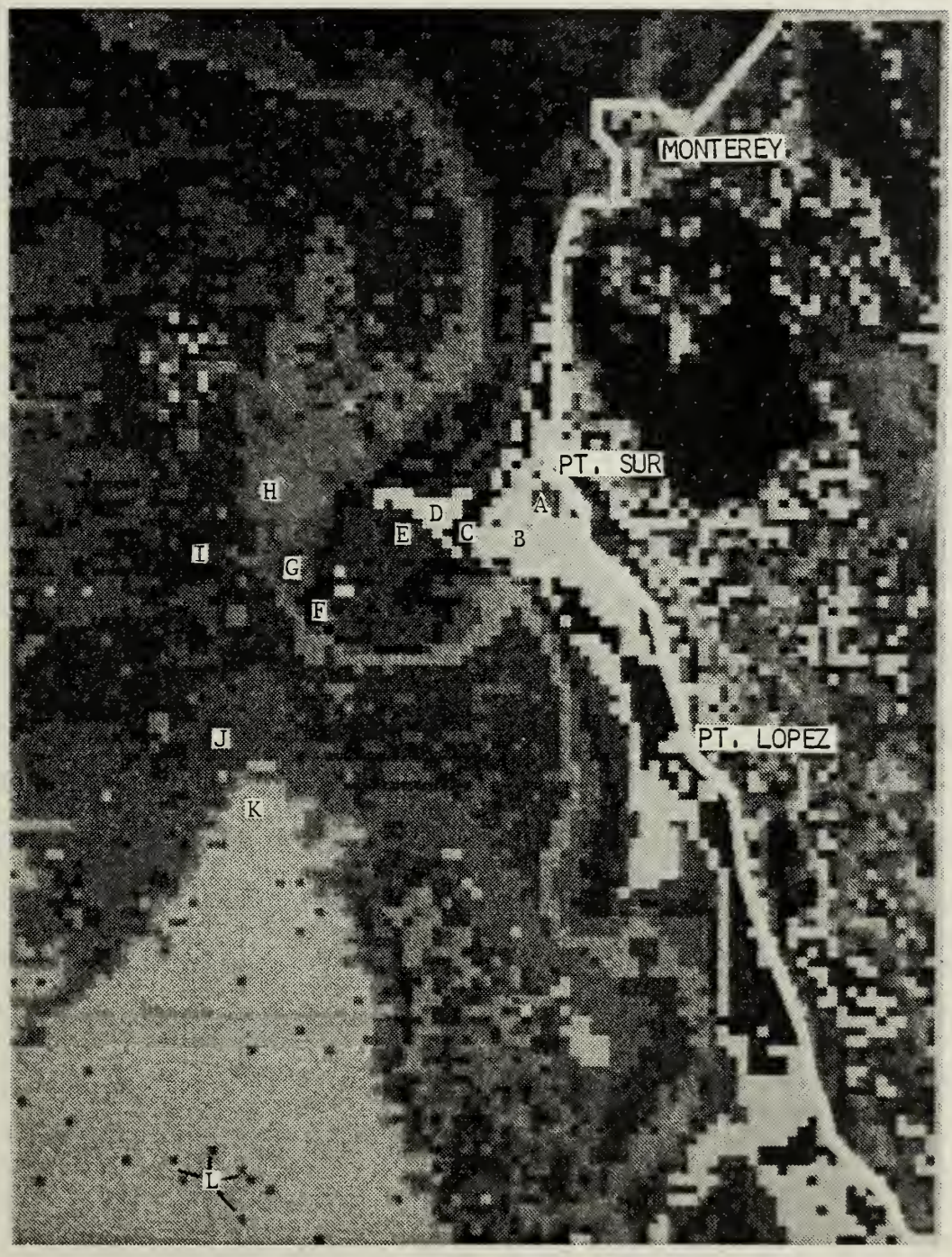

Plate 2. NOAA-6 satellite image of the California coast for 11 June 1980. Letters associated with color grades represent averaged temperatures, over a pixel, measured by the radiometer (see Table II for radiometric count, temperature, nitrate and phosphate values).

The computer printout (picprint) was also navigated, using the computer program developed by Lundell (1980), in order to draw on it the portion of the R/V ACANIA cruise track nearest in time to the satellite overpass (Fig. 9). Temperatures were digitized along the cruise track and compared with the in-situ values (Fig.10). Regression lines were computed for both in-situ and satellite temperature derived radiances, in the regions with strong gradients, viz., between elapsed distance ca. 219 km to 223 km, 223 km to 230 km and 240 km to 262 km from the comparison between these lines, averaged values for the transmittance ca. 0.525 and the path radiance ca. 3,320,000 watts·steradian^{-1}·m^{-3} were computed. Using these values in the radiative transfer equation, a calibration table for the satellite temperatures associated with the count values was constructed (Table II).

The sea surface nutrient distribution was obtained from its correlation with the in-situ thermal distribution. Linear regression analysis between nitrate and temperature, phosphate and temperature, and nitrate to phosphate yielded slopes of -4.26, -0.29 and 14.46 respectively, and y-axis intercepts of 57.67 µM, 4.85 µM and -13.54 µM respectively (Figs. 11, 12 and 13). The correlation coefficients were $r = -0.97$, $r = -0.96$ and $r = 0.99$ respectively. From this analysis a nutrient concentration was computed for each calibrated satellite temperature (Table II).

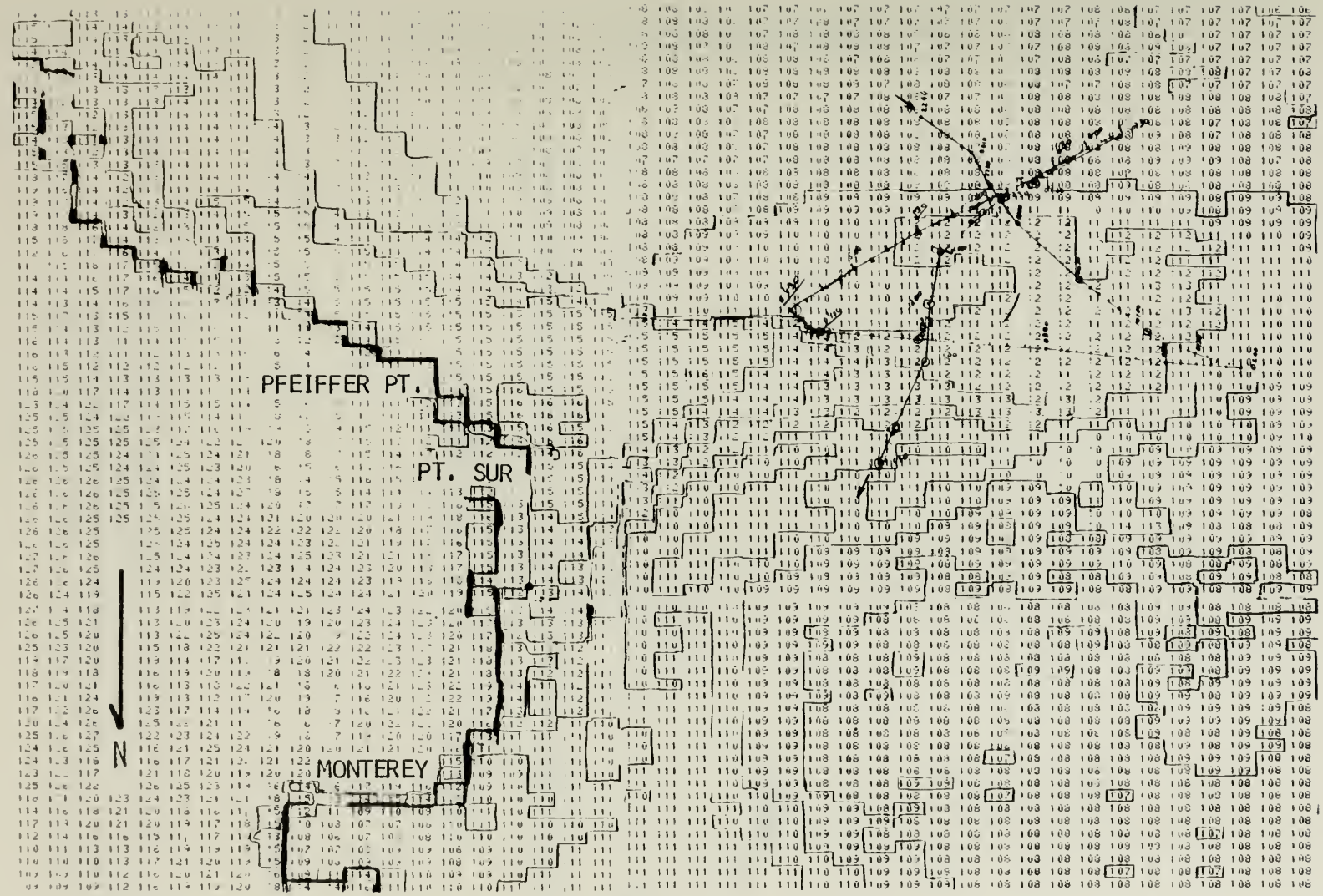

Figure 9. Sample of the picprint of the satellite image for 11 June 1980 with the coast line, thermal isolines and a portion of the June cruise drawn on it.

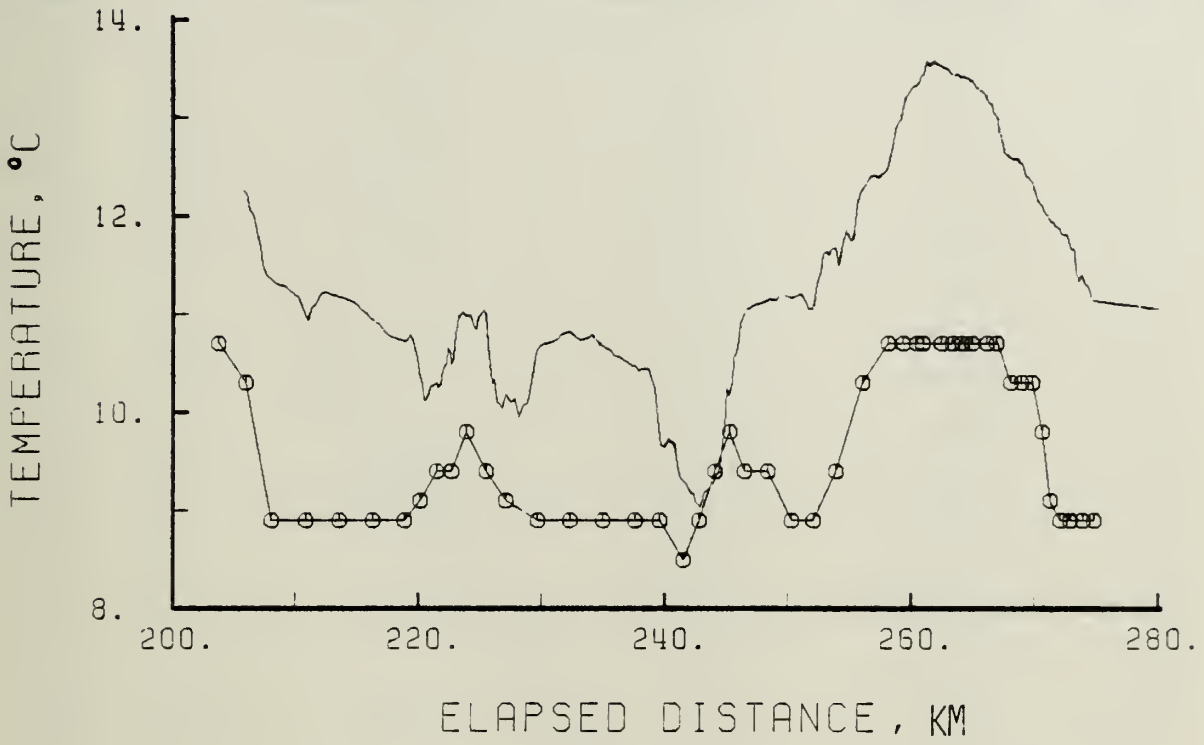

Figure 10. In-situ temperature (straight line) and satellite temperature (line with circles) versus elapsed distance along a portion of the cruise track of the 11 June 1980.

Table II

Calibration Table of the satellite image for 11 June 1980
(The '*' represents values below limit of detection)

Color Grade	Count	Satellite Temperature (°C)	Corrected Temperature (°C)	Nitrate NO_3^- (μM)	Phosphate PO_4^{3-} (μM)
L	105	12.03	15.17	*	0.48
K	106	11.59	14.48	*	0.68
J	107	11.15	13.80	*	0.87
I	108	10.70	13.10	1.82	1.07
			12.76	3.27	1.17
H	109	10.26	12.41	4.76	1.27
			12.06	6.26	1.37
G	110	9.81	11.70	7.79	1.48
			11.35	9.28	1.58
F	111	9.36	11.00	10.78	1.68
			10.65	12.27	1.78
E	112	8.91	10.29	13.80	1.88
			9.94	15.29	1.98
D	113	8.46	9.58	16.83	2.09
			9.22	18.36	2.19
C	114	8.00	8.85	19.94	2.30
			8.49	21.48	2.40
B	115	7.54	8.12	23.05	2.51
			7.76	24.59	2.61
A	116	7.08	7.39	26.17	2.72

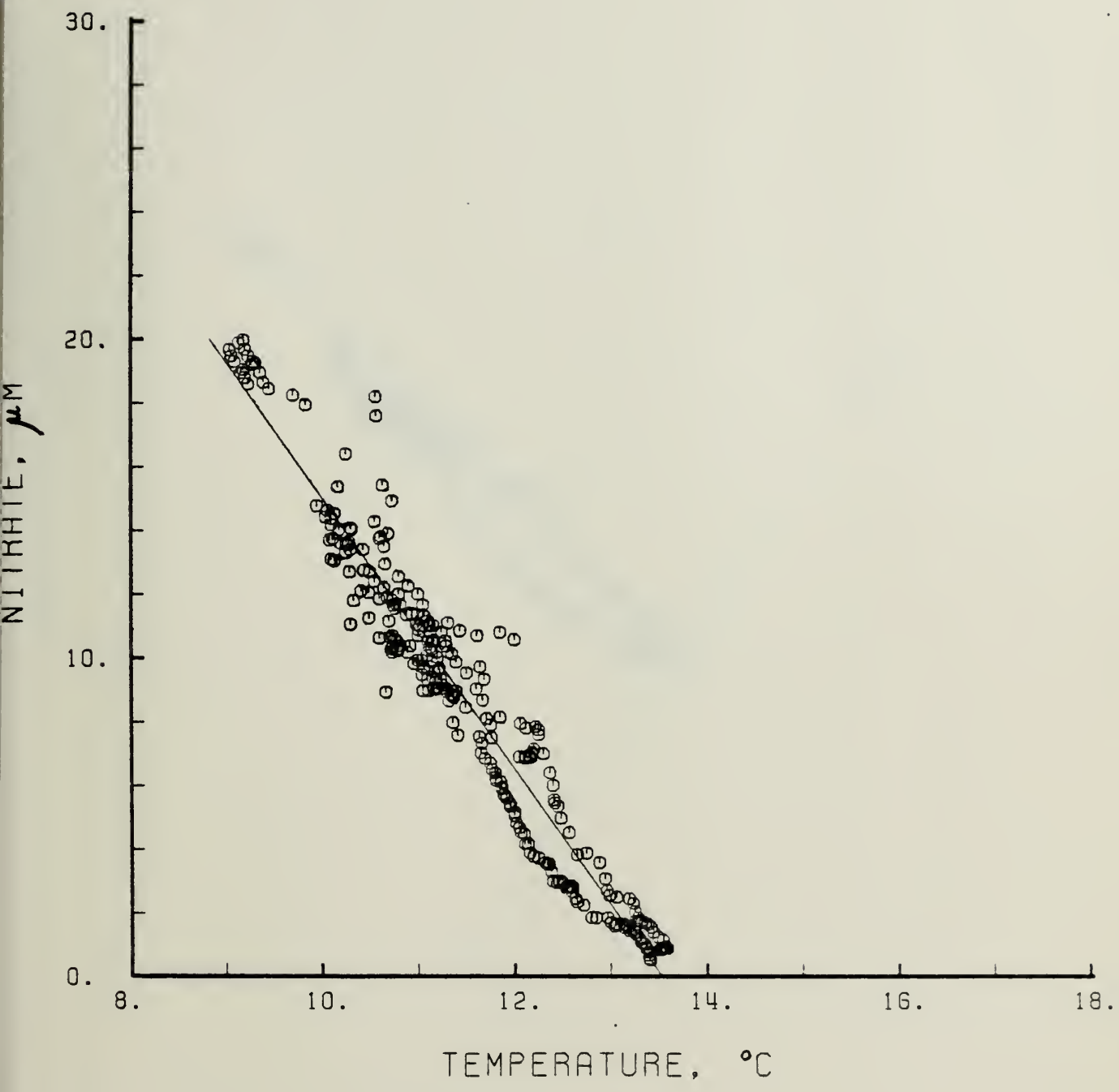

Figure 11. Nitrate versus temperature with the regression line for 11 June 1980.

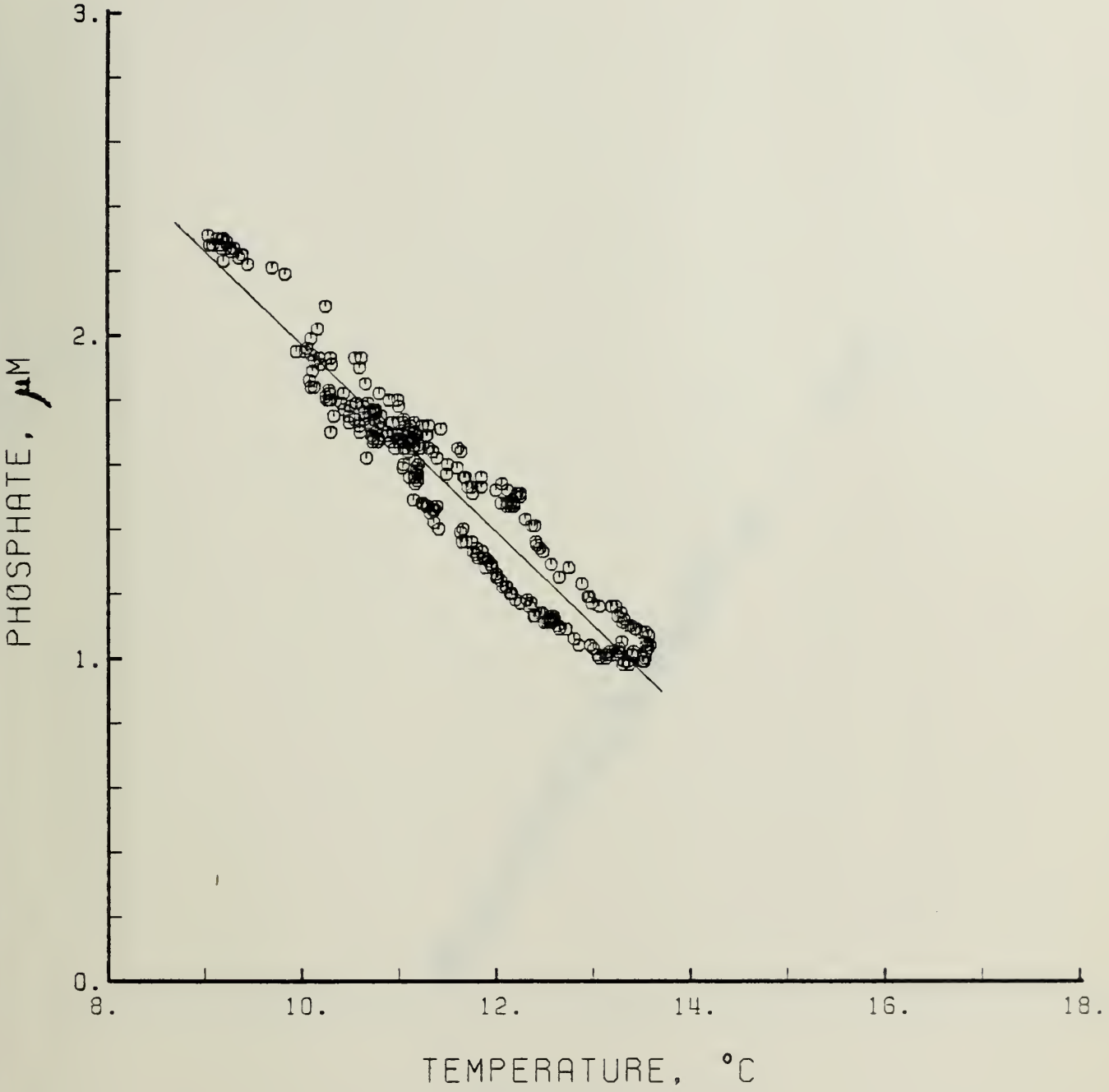

Figure 12. Phosphate versus temperature with the regression line for 11 June 1980.

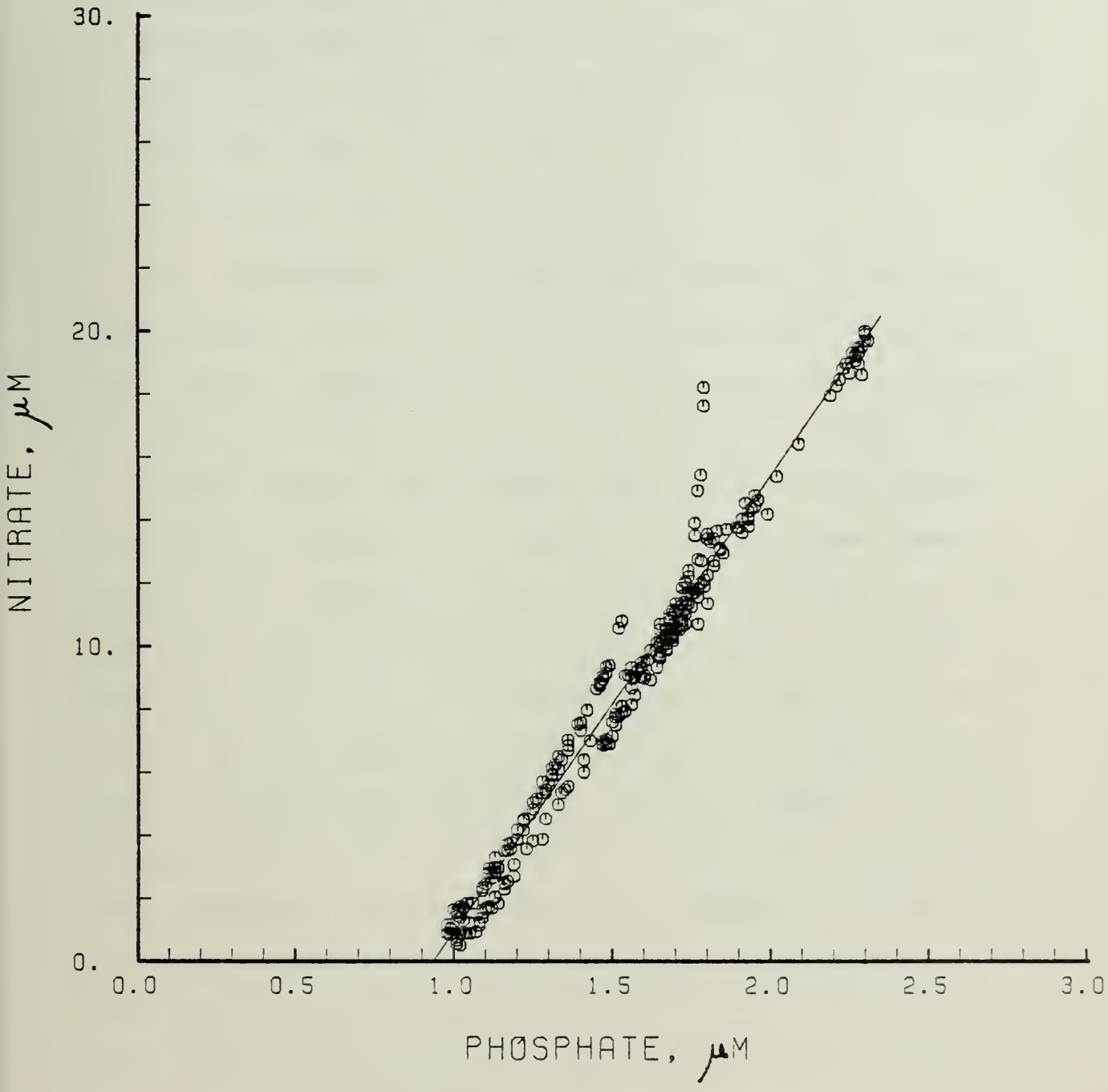

Figure 13. Nitrate versus phosphate with the regression line for 11 June 1980.

Sea surface temperature, nitrate and phosphate maps were generated by "zoom transferring"* the thermal pattern in the IR satellite image to a navigational chart. Each isopleth is the average of the temperature or nutrient concentration on each side (Figs. 14, 15 and 16).

C. 29 OCTOBER 1980 SATELLITE IMAGERY

The image taken by the satellite NOAA-6, in its orbit number 6967, at 1640 GMT 29 October 1980, shows a different cold feature, compared with the one from the June 1980 cruise. In this case, there is an elongated "tongue" of cold water.

Plate 3 shows the black and white copy of the pseudo-color image processed with IDIMS, in the NASA-Ames Research Center. The computer printout was again navigated using the computer program developed by Lundell (1980), in order to draw on it the portion of the R/V ACANIA cruise track nearest in time to the satellite overpass (Fig. 17). Temperatures were digitized along the cruise track and compared with the in-situ values (Fig. 18). Regression lines were computed for the in-situ and satellite temperature derived radiances, in the regions with strong gradients, viz., between elapsed distance ca. 21 km to 51 km, 51 km to 70 km and 170 km to 191 km. From the comparison between these lines, averaged values for the transmittance ca. 0.685 and the path radiance ca. 2,059,000 watts·steradian^{-1}·m^{-3} were computed. Using these values in the radiative transfer equation, a calibration table for

---

*See previous footnote.

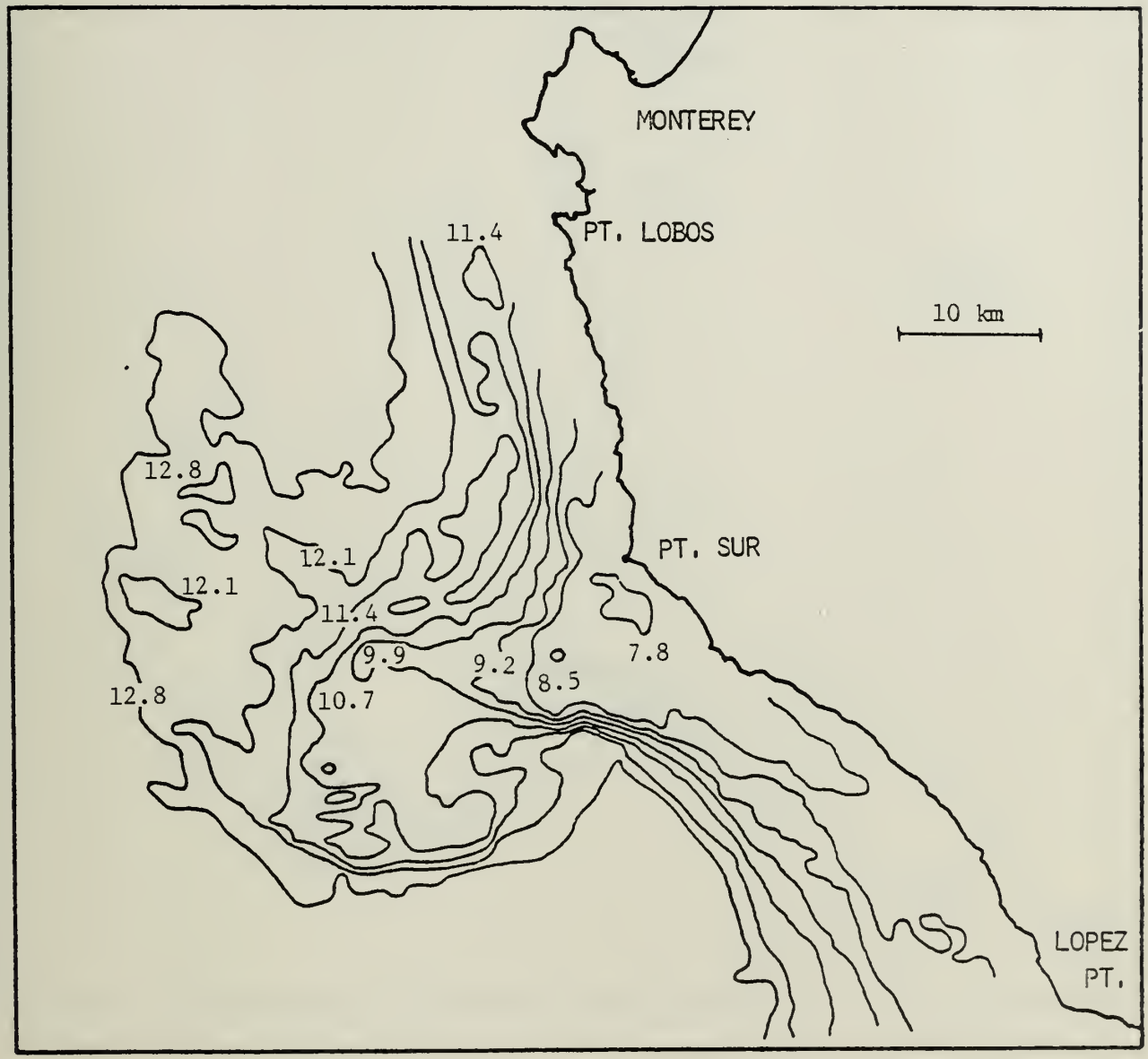

Figure 14. Sea surface temperature map in °C for 11 June 1980 inferred from satellite IR imagery. Contour interval is one radiometric unit of measurement (1 count ≃ 0.5°C).

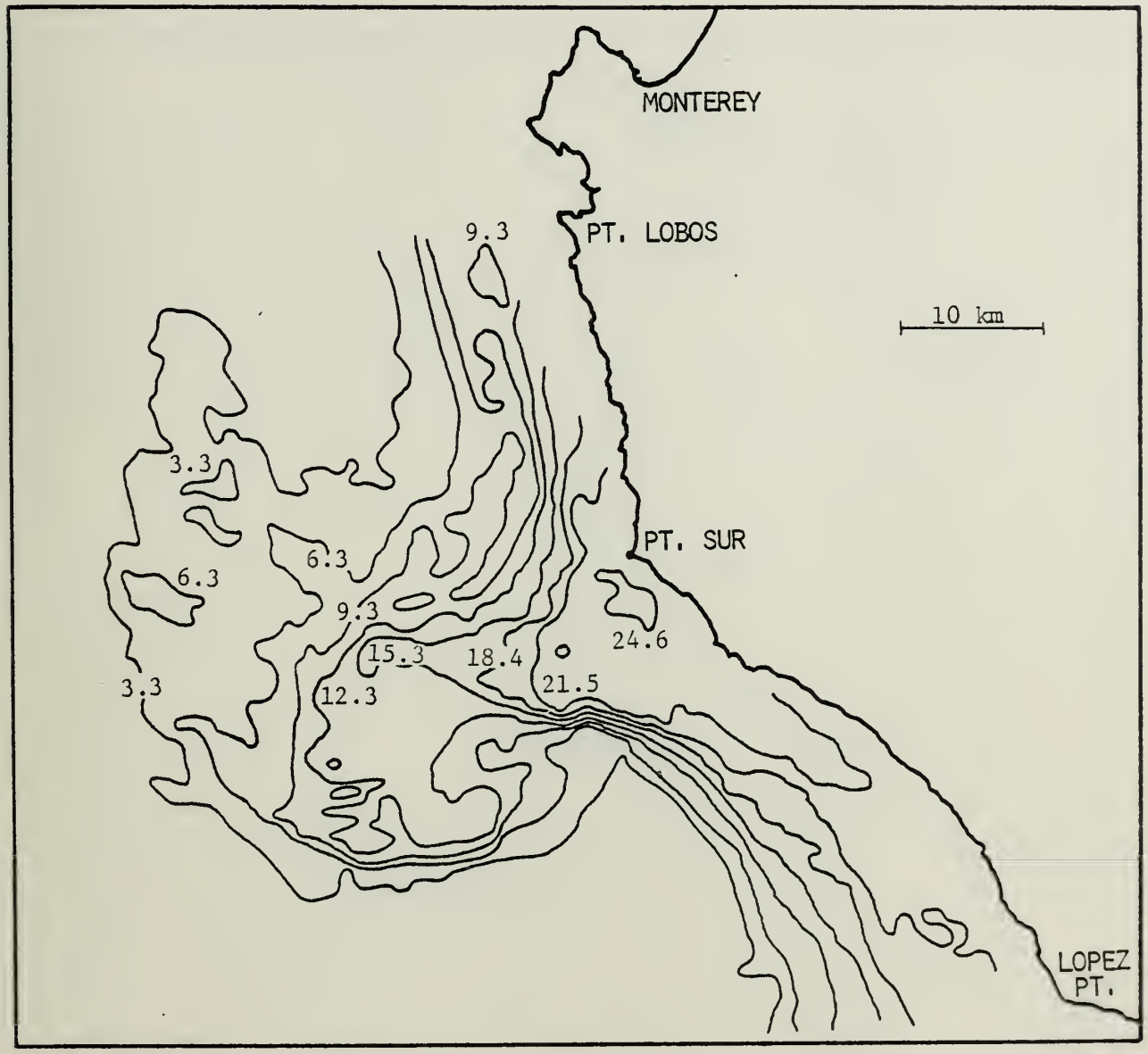

Figure 15. Sea surface nitrate map for 11 June 1980, generated by correlation with sea surface temperature distribution given by IR imagery. Contour interval is one radiometric unit of measurement (1 count ≃ 0.5°C). Nitrate concentratins given are in μM.

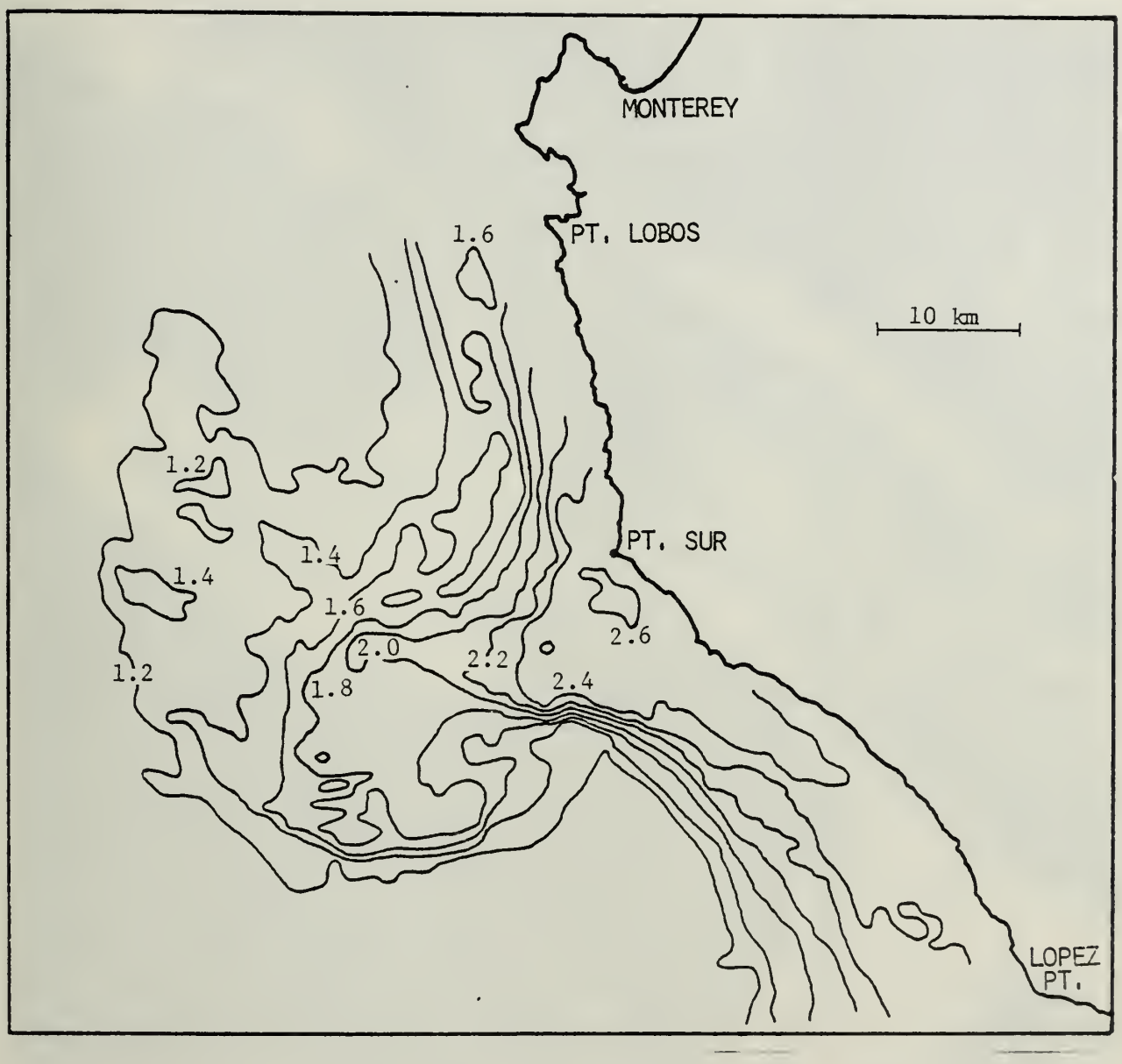

Figure 16. Sea surface phosphate map for 11 June 1980, generated by correlation with sea surface temperature distribution given by IR imagery. Contour interval is one radiometric unit of measurement (1 count ≃ 0.5°C). Phosphate concentrations are given in μM.

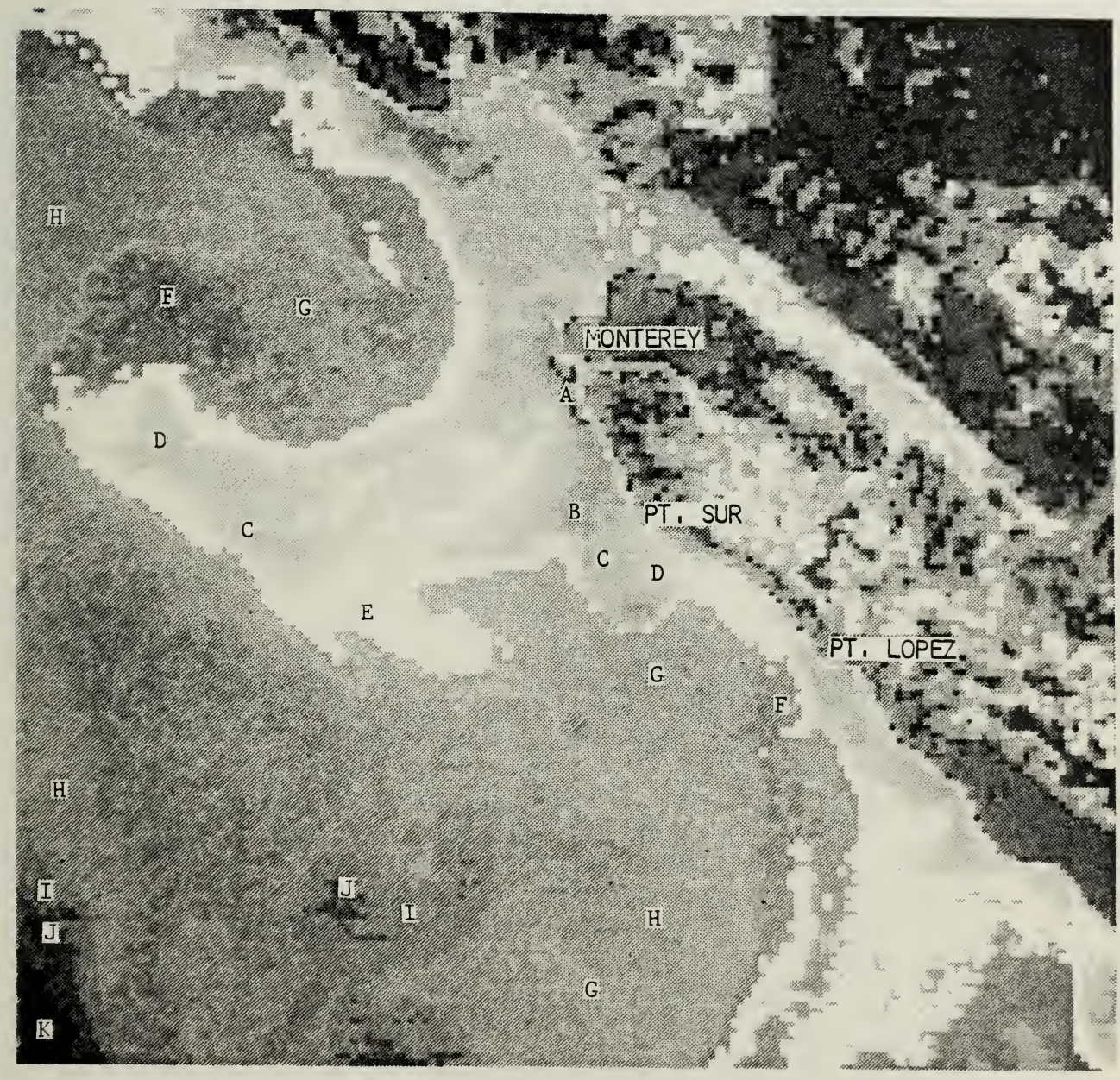

Plate 3. NOAA-6 satellite image of the California coast for 29 October 1980. Letters associated with color grades represent averaged temperatures, over a pixel, measured by the radiometer (see Table III for radiometric count, temperature, nitrate and phosphate values).

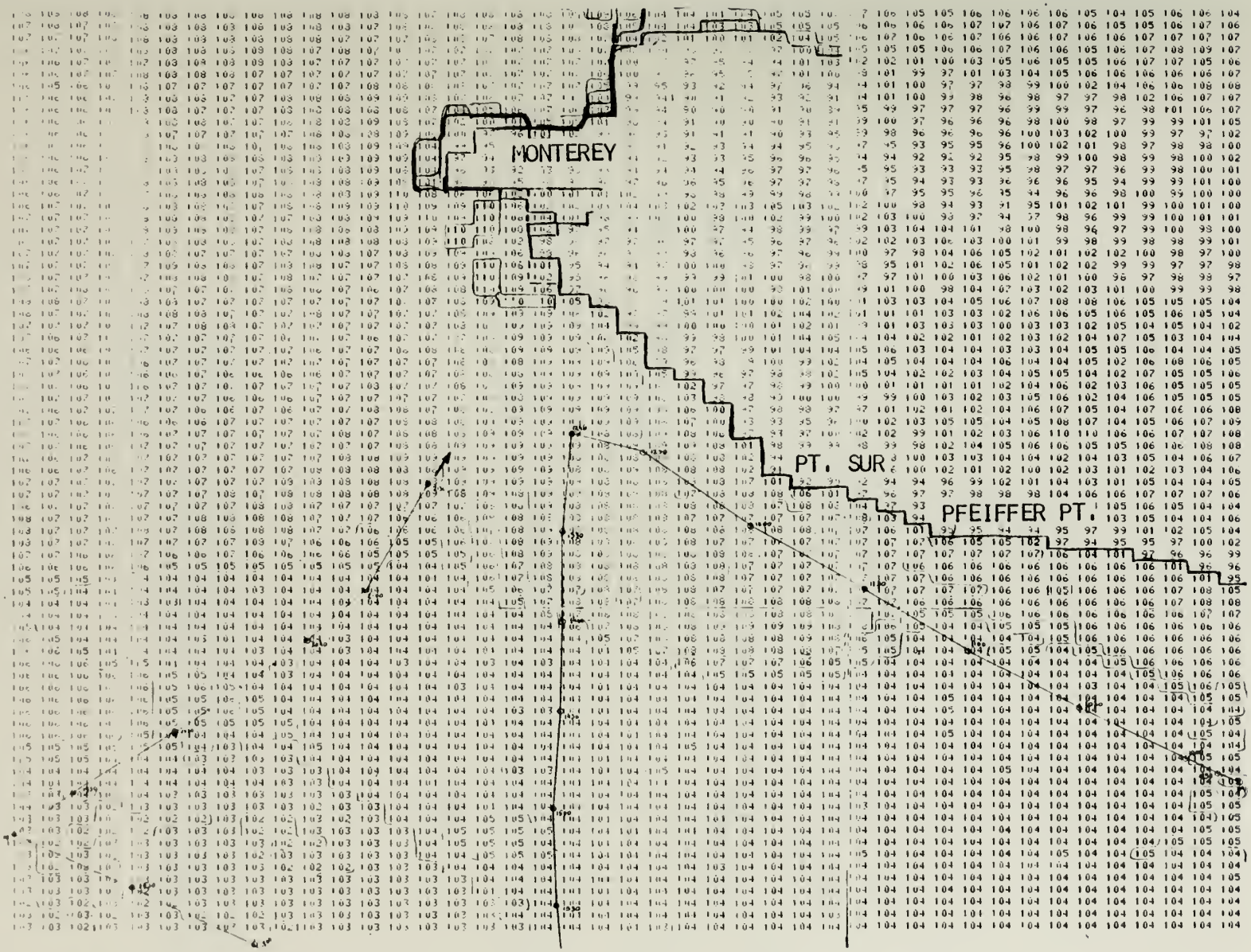

Figure 17. Sample of the picprint of the satellite image for 29 October 1980 with the coast line, thermal isolines and a portion of the June cruise drawn on it.

Figure 18. In-situ temperature (straight line) and satellite temperature (line with circles) versus elapsed distance along a portion of the cruise track of the 29 October 1980 cruise.

the satellite temperatures associated with the count values was constructed (Table III).

The sea surface nutrient distribution was obtained from its correlation with the in-situ thermal distribution. Linear regression analysis between nitrate and temperature, phosphate and temperature, and nitrate and phosphate yielded slopes of -1.27, -.09 and 13.60 respectively, and y-axis intercepts of 25.26 μM, 2.26 μM and -6.94 μM respectively (Figs. 19, 20 and 21). The correlation coefficients were $r = -0.71$, $r = -0.70$ and $r = 0.94$ respectively. From this analysis a nutrient concentration was computed for each calibrated satellite temperature (Table III).

Sea surface temperature, nitrate and phosphate maps were generated by "zoom transferring" the thermal pattern in the IR satellite image to a navigational chart. Each isopleth is the average of the nutrient or nutrient concentration on each side (Figs. 22, 23 and 24).

Table III

Calibration table of the satellite image for 29 October 1980

Color Grade	Count	Satellite Temperature (°C)	Corrected Temperature (°C)	Nitrate NO_3^- (μM)	Phosphate PO_4^{3-} (μM)
K	100	14.20	18.49	1.83	0.67
J	101	13.77	17.89	2.59	0.73
I	102	13.34	17.28	3.36	0.78
H	103	12.90	16.66	4.15	0.83
G	104	12.47	16.06	4.91	0.88
F	105	12.03	15.44	5.70	0.94
			15.13	6.10	0.96
E	106	11.59	14.81	6.49	0.99
			14.50	6.89	1.02
D	107	11.15	14.19	7.28	1.04
			13.87	7.69	1.07
C	108	10.70	13.55	8.09	1.10
			13.24	8.49	1.13
B	109	10.26	12.93	8.88	1.15
			12.61	9.29	1.18
A	110	9.81	12.28	9.70	1.21

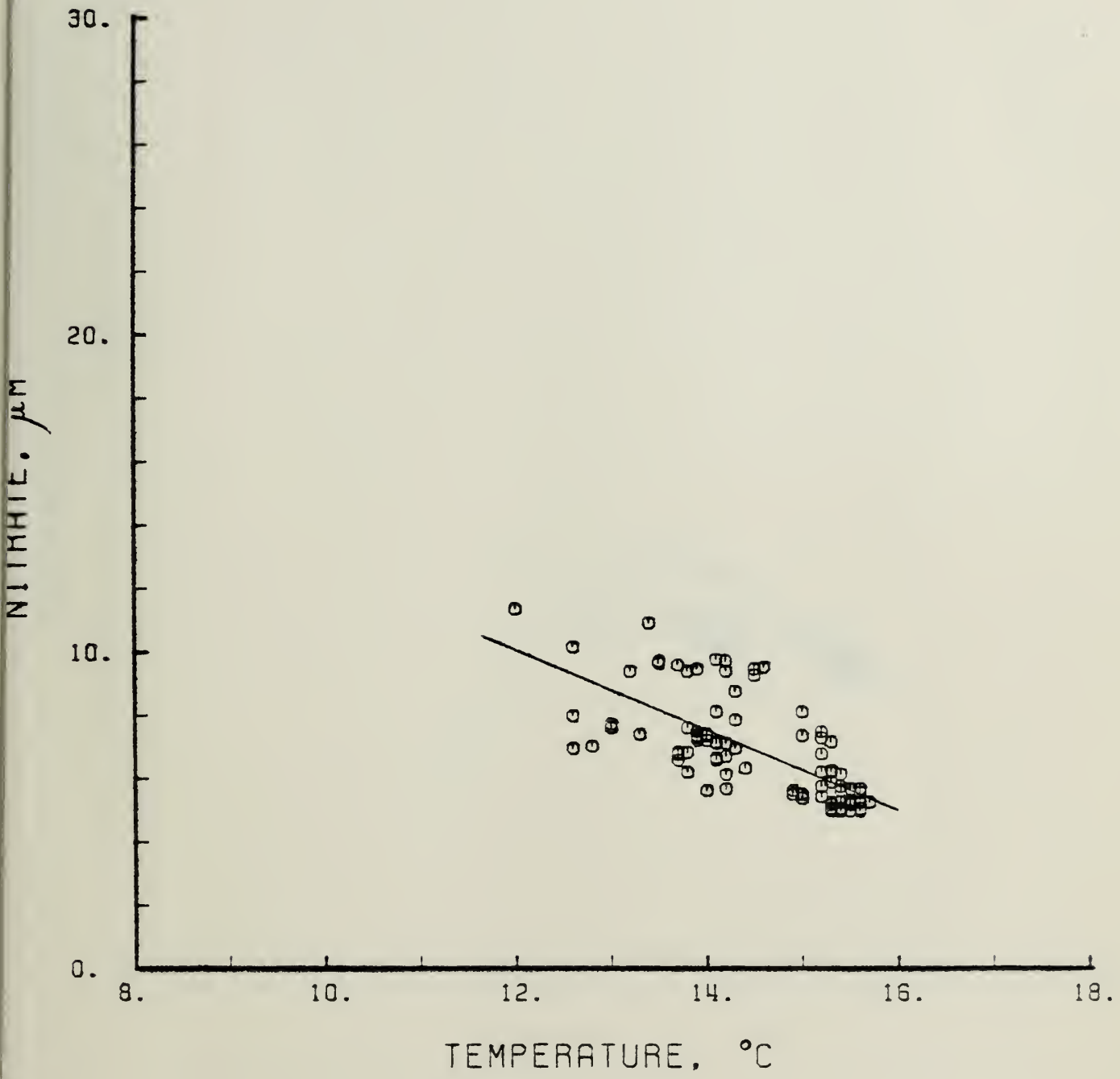

Figure 19. Nitrate versus temperature with the regression line for 29 October 1980.

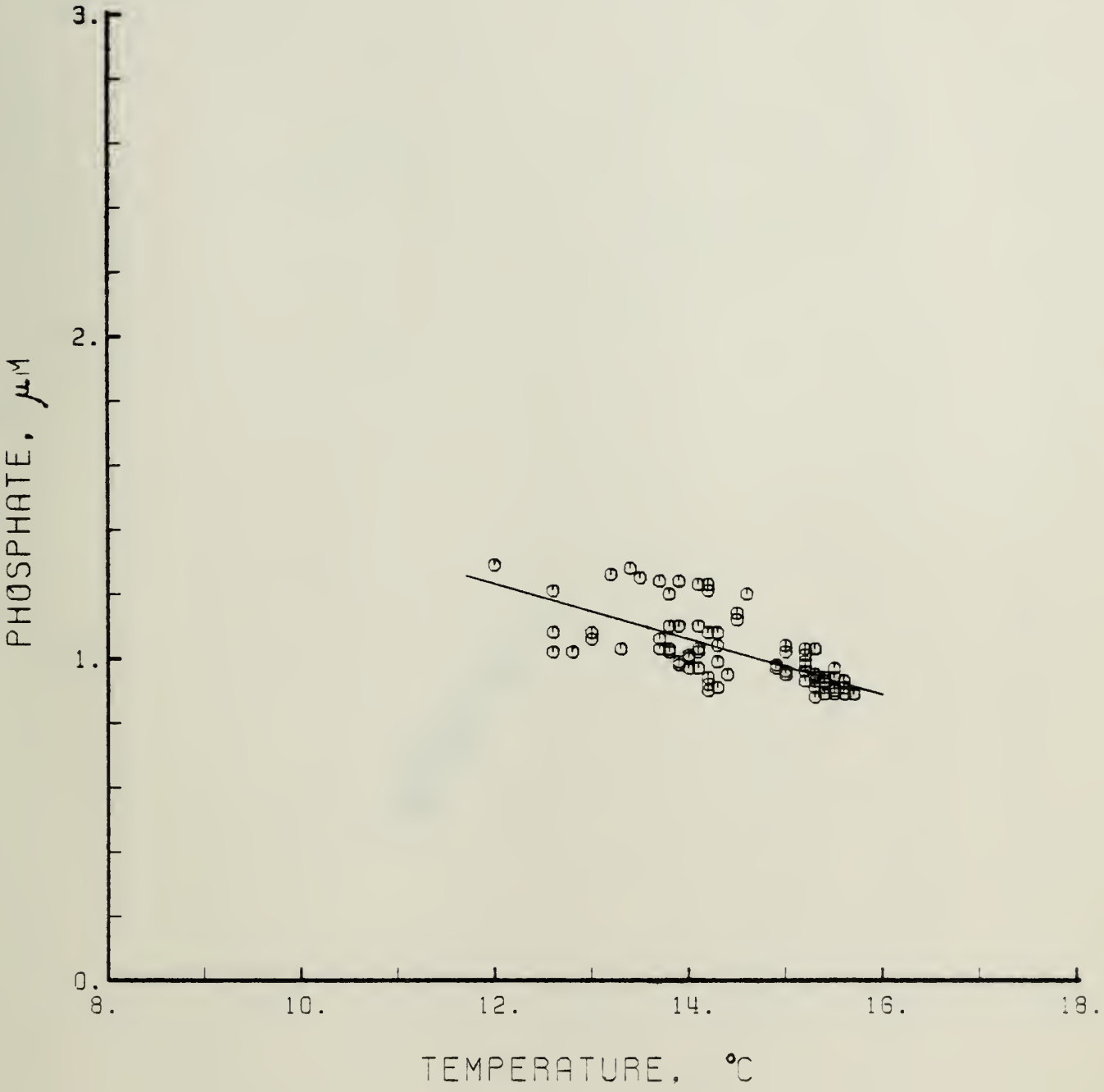

Figure 20. Phosphate versus temperature with the regression line for 29 October 1980.

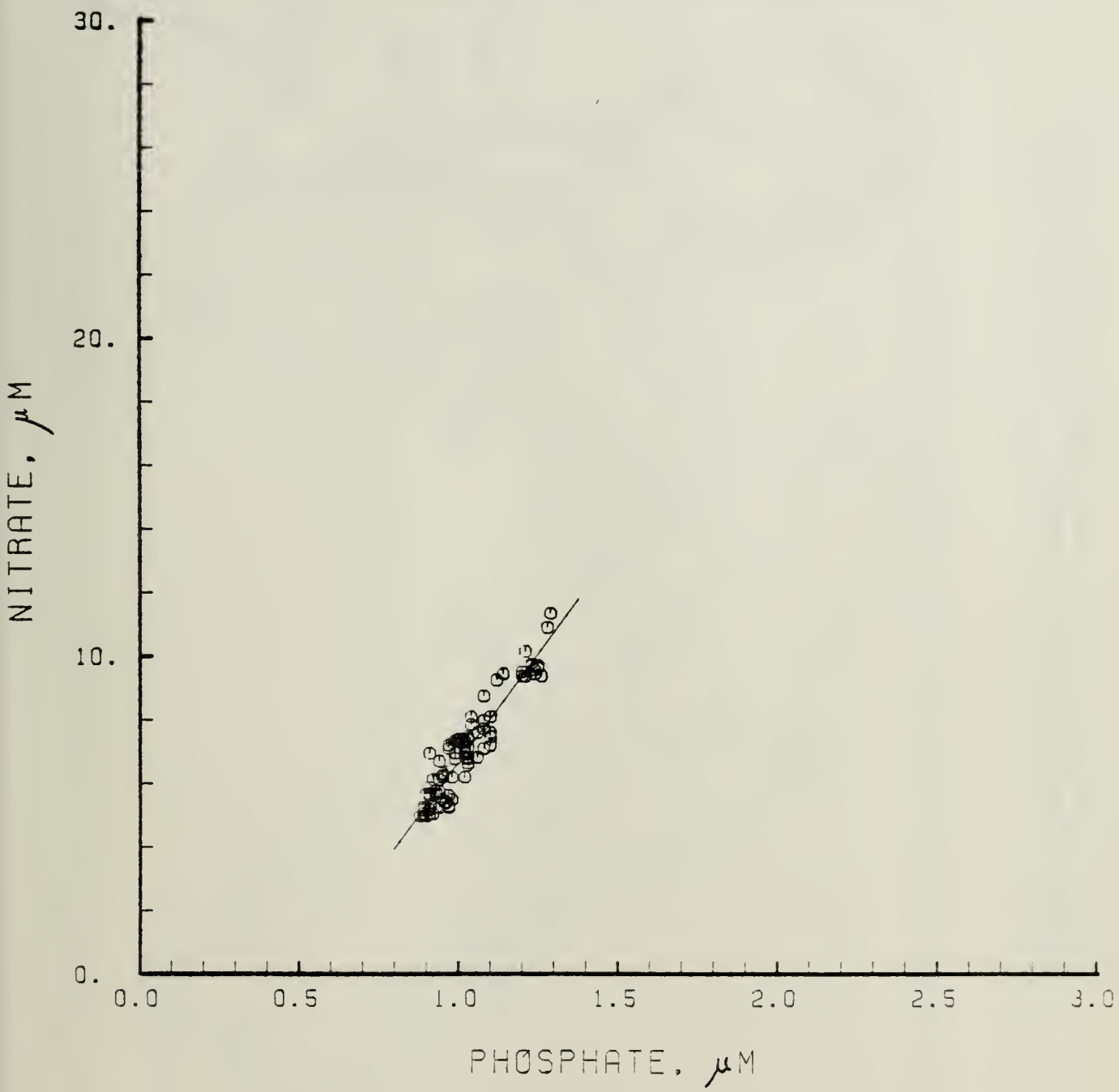

Figure 21. Nitrate versus phosphate with the regression line for 29 October 1980.

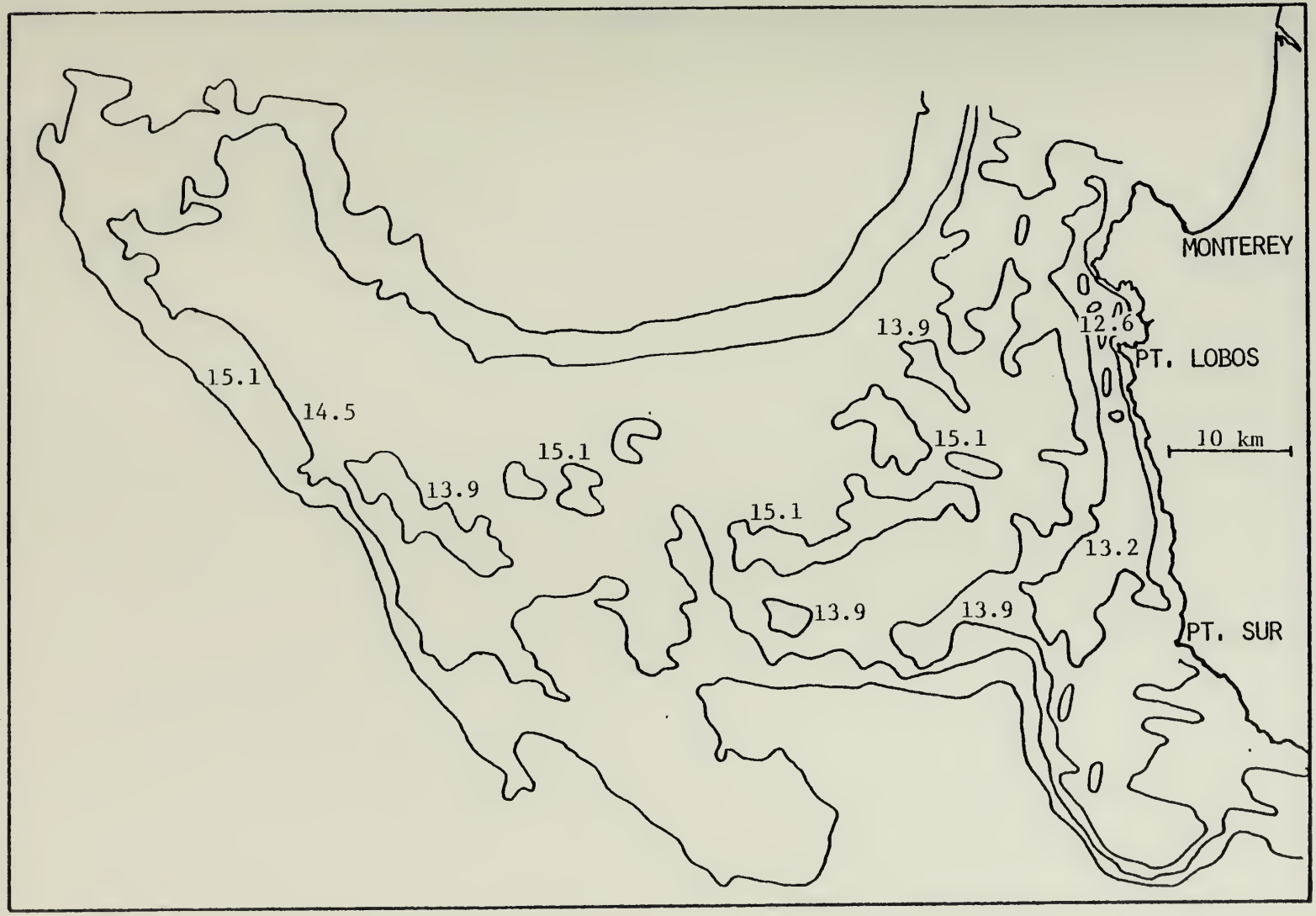

Figure 22. Sea surface temperature map in °C for 29 October 1980 inferred from satellite IR imagery. Contour interval is one radiometric unit of measurement (1 count ≃ 0.5°C).

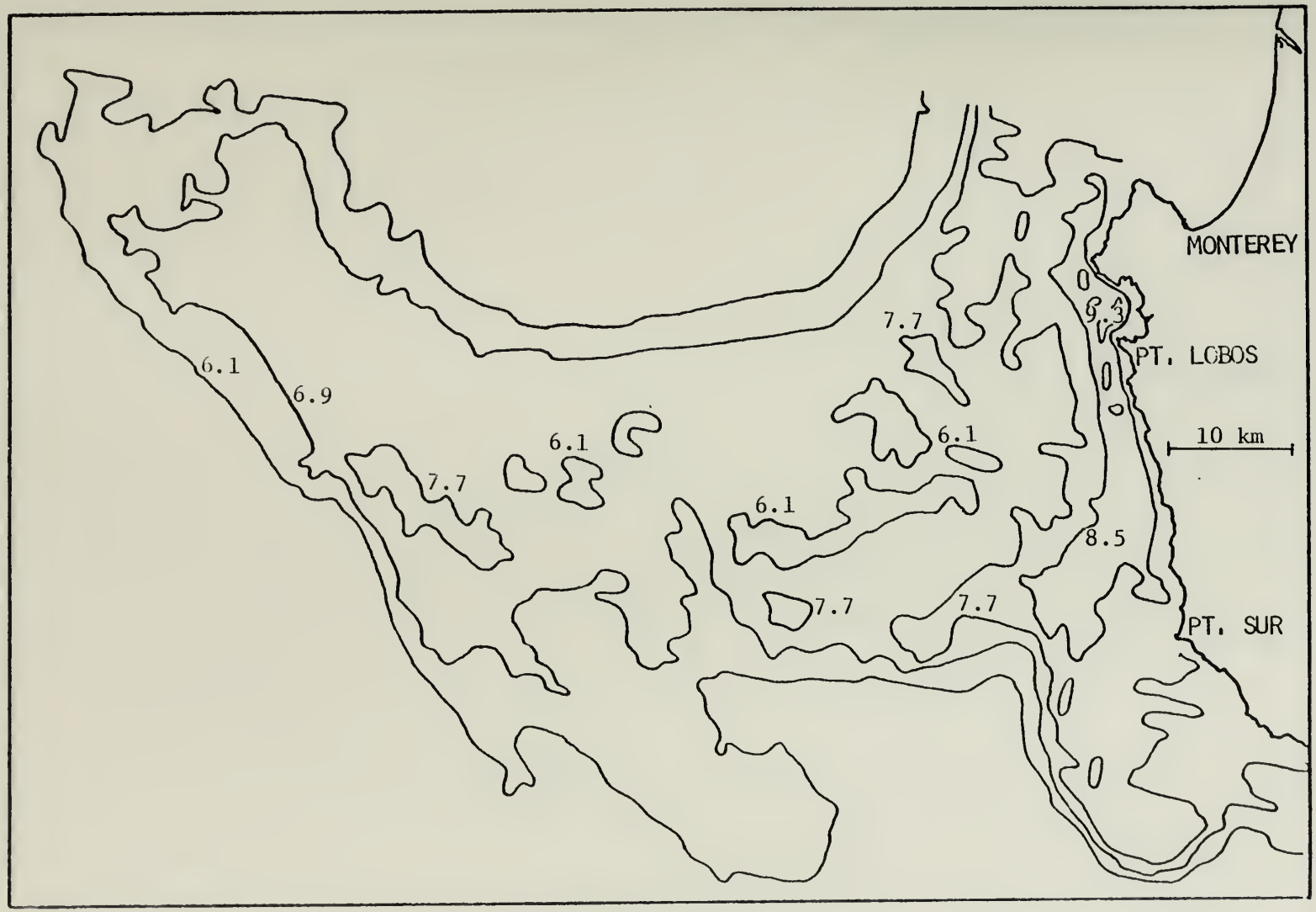

Figure 23. Sea surface nitrate map for 29 October 1980, generated by correlation with sea surface temperature distribution given by IR imagery. Contour interval is one radiometric unit of measurement (1 count ≃ 0.5°C). Nitrate concentrations are given in μM.

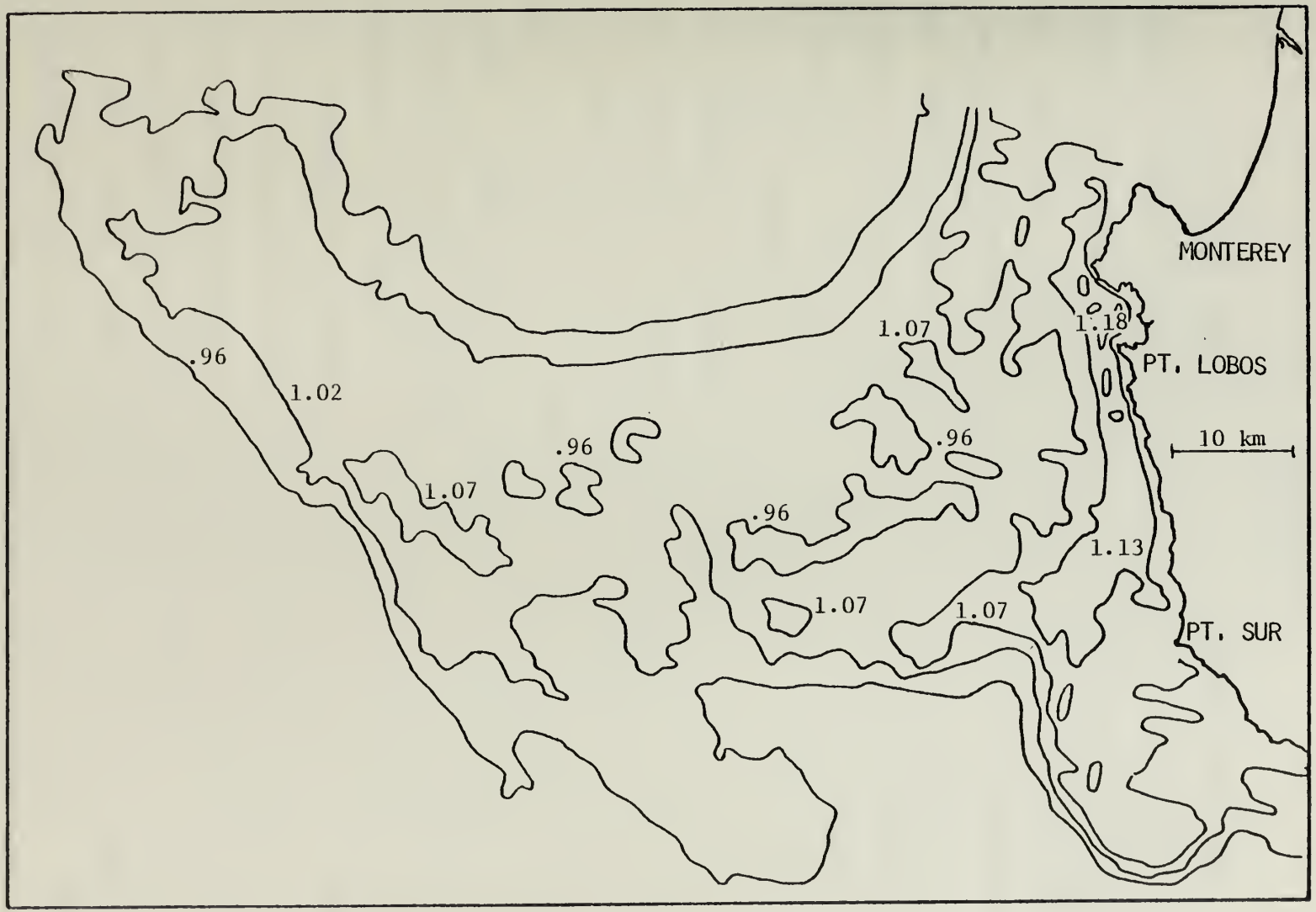

Figure 24. Sea surface phosphate map for 29 October 1980, generated by correlation with sea surface temperature distribution given by IR imagery. Contour interval is one radiometric unit of measurement (1 count ≃ 0.5°C). Nitrate concentrations are given in μM.

IV. DISCUSSION

Inferring sea surface nutrient concentrations from satellite derived thermal patterns appears feasible in regions of strong upwelling, where the nutrients to temperature correlations are very high. However, some errors are to be expected. The computer program developed by Lundell (1980) to navigate on the picprint can introduce an error in the position of the cruise track on the order of two lines and two pixels apart (distance ~ 2 km) [Lundell, 1980]. With the identification of three landmarks (Pt. Sur, Pfeiffer Pt. and Pt. Lopez) on the picprint, the author could compute a r.m.s. error of ca. 0.9 lines and 1.3 pixels for the 9 June 1980 cruise track, ca. 1.0 lines and 2.1 pixels for the 11 June 1980 cruise track, ca. 0.8 lines and 1.8 pixels for the 29 October 1980 cruise track. These errors are smaller than expected due to the proximity of the landmarks, and they will not significantly influence the accuracy of the thermal calibration. However, the process of averaging the transmittance and path radiance values obtained for each sharp temperature gradient along the portion of the cruise track will add a significant error. Taking this into account, the author computed a std. dev. ±0.25°C, ±0.13 °C and ±0.56°C for the calibrated temperature values on 9 June 1980, 11 June 1980 and 29 October 1980, respectively. From these values we can conclude that the temperature accuracy increases if we apply the radiative

transfer equation in regions with sharp temperature gradients, as in upwelling fronts. With these errors for the thermal maps, it would be expected to find errors of 9% and 4% for the nitrate and phosphate values in the maps respectively, on 9 June 1980, 3% and 2% for the nitrate and phosphate values in the maps respectively, on 11 June 1980, and 8% and 10% for the nitrate and phosphate values in the maps respectively, on 29 October 1980. Also, there are small additional errors due to imperfect temperature vs. nutrients correlations, that are negligible when applied in regions of strong upwelling. The quality and the accuracy of the results depends upon the uniformity of the age of the upwelled surface waters (compare correlation values in June and October, in Table IV). It therefore seems reasonable to assume that in an upwelling zone, the major patterns of nutrient concentrations can be inferred using satellite IR imagery and limited in-situ thermal and nutrient data, and even be used in the construction of a biochemical model, or further, of a predictive model in frontal zones.

TABLE IV

Summary Table of Nutrients vs.
Temperature Linear Regression
Analysis

DAY	Linear Regression Equations N - nitrate (μM) P - phosphate (μM) T - Temperature (°C)	Correlation
9 June	N = -3.55T + 49.27	-0.96
	P = -0.27T + 4.72	-0.96
11 June	N = -4.26T + 57.67	-0.97
	P = -0.29T + 4.85	-0.96
29 October	N = -1.27T + 25.26	-0.71
	P = -0.09T + 2.26	-0.70

LIST OF REFERENCES

1. Traganza, E.D., "Satellite and Synoptic Studies of Chemical Mesoscale Processes in the Upper Layer." Proposal for Research submitted to the Office of Naval Research (ONR) Code 482, NSTL, Bay St. Louis, MO 39529.

2. Traganza, E.D., Nestor, D.A., and McDonald, A.K., "Satellite Observations of a Nutrient Upwelling off the Coast of California," Journal of Geophysical Research, V. 85 (C7), p. 4101-4106, 1980.

3. Bowman, M.J., et al., "Oceanic Fronts in Coastal Processes," Proceedings of a Workshop held at the Marine Sciences Research Center. May 25-27, p. 2-5, 1977.

4. Traganza, E.D., Conrad, J.W., and Breaker, L.C., "Satellite Observations of a 'Cyclonic Upwelling System' and 'Giant Plume' in the California Current," Coastal Upwelling, American Geophysical Union, 2000 Florida Ave., N.W. Washington, D.C. 20009, 1981.

5. Eppley, R.W., Renger, E.H., Harrison, W.G., "Nitrate and phytoplankton production in southern California coastal waters," Limnology and Oceanography, V. 24, p. 483-494, 1979.

6. Traganza, E.D., Austin, D., "Nutrient mapping and the biological structure of upwelling systems from satellite infrared and ocean images," Science (1981) (in process).

7. Hovis, W.A., et al., Science 210, 6 (1980).

8. Hanson, W.E., "Nutrient Study of Mesoscale Thermal Features off Point Sur, California," M.S. Thesis, Naval Postgraduate School, Monterey, California, 1975.

9. Lundell, G., "Rapid Oceanographic Data Gathering: Some problems in using remote sensing to determine the horizontal and vertical thermal distributions in the northeast Pacific Ocean," M.S. Thesis, Naval Postgraduate School, Monterey, California, 1981.

10. Maul, G.A., and Sidrin, M., "Atmospheric Effects on Ocean Surface Temperature Sensing from the NOAA Satellite Scanning Radiometer," Journal of Geophysical Research, V. 18 (12), p. 1909, 1973.

11. Maul, G.A., et al., "Geostationary satellite observations of Gulf Stream meanders: infrared measurements and time series analysis," Journal of Geophysical Research, 83 (C13), p. 6123-6135, 1978.

12. Stewart, R., "Notes on Satellite Oceanography," Scripps Institution of Oceanography, 1979.

INITIAL DISTRIBUTION LIST

		No. Copies
1.	Defense Technical Information Center Cameron Station Alexandria, Virginia 22314	2
2.	Library, Code 0142 Naval Postgraduate School Monterey, California 93940	2
3.	Chairman, Code 68Mr Department of Oceanography Naval Postgraduate School Monterey, California 93940	1
4.	Chairman, Code 63Rd Department of Meteorology Naval Postgraduate School Monterey, California 93940	1
5.	Dr. E.D. Traganza, Code 68Tg Department of Oceanography Naval Postgraduate School Monterey, California 93940	7
6.	LT. C.D. Jori NORDA NSTL Station Bay St. Louis, Mississippi 39529	1
7.	Director Naval Oceanography Division Naval Observatory 34th & Massachusetts Avenue NW Washington, D.C. 20390	1
8.	Commander Naval Oceanography Command NSTL Station Bay St. Louis, Mississippi 39529	1
9.	Commanding Officer Naval Oceanographic Office NSTL Station Bay St. Louis, Mississippi 39529	1

10. Commanding Officer — 1
Fleet Numerical Oceanography Center
Monterey, California 93940

11. Commanding Officer — 1
Naval Ocean Research & Development Activity
NSTL Station
Bay St. Louis, Mississippi 39529

12. Office of Naval Research (Code 482) — 1
Naval Ocean Research & Development Activity
NSTL Station
Bay St. Louis, Mississippi 39529

13. Scientific Liaison Office — 1
Office of Naval Research
Scripps Institution of Oceanography
La Jolla, California 92037

14. Library — 1
Scripps Institution of Oceanography
P.O. Box 2367
La Jolla, California 92037

15. Library — 1
Department of Oceanography
University of Washington
Seattle, Washington 98105

16. Library — 1
CICESE
P.O. Box 4803
San Ysidro, California 92073

17. Office of Naval Research (Code 480) — 1
Naval Ocean Research and Development Activity
NSTL Station
Bay St. Louis, Mississippi 39529

18. Chief of Naval Research — 1
800 N. Quincy Street
Arlington, Virginia 22217

19. Commanding Officer — 1
Naval Environmental Prediction Research Facility
Monterey, California 93940

20. Chairman, Oceanography Department — 1
U.S. Naval Academy
Annapolis, Maryland 21402

21. Mr. Ben Cagle — 1
Office of Naval Research Branch Office
1030 East Green Street
Pasadena, California 91106

22. Dr. Robert E. Stevenson — 1
Scientific Liaison Office, ONR
Scripps Institution of Oceanography
La Jolla, California 92037

23. Ms. Bonita Hunter, Code 68 — 1
Department of Oceanography
Naval Postgraduate School
Monterey, California 93940

24. LCDR Craig S. Nelson — 1
Pacific Environmental Group
c/o FNOC
Monterey, California 93940

25. Dr. Edward Green — 1
Office of Naval 102 Research (Code 482)
Ocean Sciences & Technology Division
Chemical Oceanography Program
NSTL Station
Bay St. Louis, Mississippi 39529

26. Lt. Vitor Silva — 3
Instituto Hidrografico
Rua das Trinas, 39
Lisbon, PORTUGAL

27. Dr. J. L. Mueller, Code 68My — 1
Department of Oceanography
Naval Postgraduate School
Monterey, CA 93940

Thesis
S49417 Silva
c.1
199097
Thermal calibration of satellite infrared images and correlation with sea-surface nutrient distribution.